The role of multiscale interaction in the maintenance and propagation of MJO in boreal winter

Jiwang Ma[a,b,c], X. San Liang[a,b,d], Dake Chen[a]

[a] *Division of Frontier Research, Southern Marine Science and Engineering Guangdong Laboratory (Zhuhai), Zhuhai, China*

[b] *Department of Atmospheric and Oceanic Sciences, Fudan University, Shanghai, China*

[c] *Shandong Meteorological Observatory, Jinan, China*

[d] *IRDR ICoE on Risk Interconnectivity and Governance on Weather/Climate Extremes Impact and Public Health, Fudan University, Shanghai, China*

Corresponding author: X. San Liang, xsliang@fudan.edu.cn

File generated with AMS Word template 2.0

Early Online Release: This preliminary version has been accepted for publication in *Journal of Climate*, may be fully cited, and has been assigned DOI 10.1175/JCLI-D-23-0332.1. The final typeset copyedited article will replace the EOR at the above DOI when it is published.

ABSTRACT

The multiscale interaction and its role in the maintenance and propagation of the Madden-Julian Oscillation (MJO) has been investigated using the newly developed multiscale window transform (MWT), the theory of canonical transfer, and the MWT-based multiscale energetics analysis (here particularly for this study, dry energetics analysis). The field variables are reconstructed/filtered with MWT onto three scale windows, namely, high-frequency window, intraseasonal window and low-frequency window. Compositing the intraseasonal fields with respect to the real-time multivariate MJO (RMM) index unambiguously shows that the zonal extents of the easterlies and westerlies of MJO vary with the RMM phases, among which phases 4 and 2 are representative. In the former phase, MJO has easterlies and westerlies within the same extent, while in the latter their extents are quite different. In phase 4, besides the previously discovered mechanisms such as pressure work and buoyancy conversion, MJO is also energized by the canonical kinetic energy (KE) transfer from the low-frequency window to the intraseasonal window (signifying barotropic instability) on the west of its convection. But on the eastern side, MJO loses KE to the low-frequency window. The KE transport also functions like an energy sink. In phase 2, the MJO variabilities can be divided into an Eastern part and a Western part. The former is essentially the same as that in phase 4; for the latter, barotropic instability dominates. On the available potential energy (APE) budget, baroclinic instability and intraseasonal APE transport help produce and maintain the temperature anomalies. In contrast to previous energetics studies, our findings highlight the essential role played by multiscale interactions.

1. Introduction

The Madden-Julian Oscillation, or MJO for short, is the dominant intraseasonal signal in the tropics and behaves as a slowly eastward-propagating system, in which the circulation, convection, and thermodynamical structures are coupled as a whole from India Ocean through Western Pacific. Enormous attention has been paid to it since its discovery by Madden and Julian (1971) and by Hsieh et al. (1963) independently (Li et al. 2018). It has profound influences to the ambient weather (e.g., Lau and Chan 1986; Hendon and Liebmann

Accepted for publication in *Journal of Climate*. DOI 10.1175/JCLI-D-23-0332.1.

1990; Mo and Higgins 1998; Paegle et al. 2000; Matthews 2004) and many other atmospheric processes, such as typhoons (e.g., Liebmann et al. 1994; Maloney and Hartmann 2001; Kim et al. 2008; Chen et al. 2009; Hsu et al. 2010), El Niño-Southern Oscillation (ENSO) (e.g., Weickmann 1991; Kessler et al. 1995; Moore and Kleeman 1999; Kessler and Kleeman 2000; Tang and Yu 2008), monsoons (e.g., Krishnamurti and Subrahmanyam 1982; Chen and Chen 1995; Zhou and Chan 2005; Straub et al. 2006; Tong et al. 2009; Chi et al. 2015), atmospheric blocking (e.g., Cassou 2008; Moore et al. 2010; Hamill and Kiladis 2014; Henderson et al. 2016), to name several. Though the importance of MJO in the climate and weather systems is well recognized, the ability of simulating it in state-of-the-art dynamic models remains limited, in spite of the advances in the past few decades (e.g., Jiang et al. 2015). Jiang et al. (2015) also show that only one fourth of the models well simulate its systematic eastward propagation.

Understanding the dynamics underlying MJO is an essential task to improve the capabilities of models in MJO simulation. Lots of theories have been proposed to understand the core dynamics from the aspect of coupling the circulation and moist processes. This line of work includes, on an incomplete list, the theories of wave-CISK (Lindzen 1974; Lau and Peng 1987; Chang and Lim 1988; Wang 1988), wind-induced surface heat exchange (Emanuel 1987; Yano and Emanuel 1991)/wind-evaporation feedback (Neelin et al. 1987), trio-interaction (Wang et al. 2016), moisture mode (Fuchs and Raymond 2005; Raymond and Fuchs 2009; Sobel and Maloney 2012; Adames and Kim 2016; Wang and Sobel 2022), skeleton (Majda and Stechmann 2009), gravity wave (Yang and Ingersoll 2013), and large-scale "convective vortex" (Hayashi and Itoh 2017), etc. However, some recent studies argue that moist processes may not be a necessary factor in the MJO dynamics if nonlinearity of the circulation is considered (Yano and Tribbia 2017). They show that the scale and phase velocity of the simulated "modon" in a dry global shallow-water model are consistent with the observed features. The diversity in theory echoes the complexity in dynamics, which may partially account for the challenge in MJO simulation.

Among the dynamics issues of MJO, the role of multiscale interaction is an important one. Multiscale interactions during MJO have been examined in many previous works, e.g., Maloney and Hartmann (1998, 2000, 2001); Hagos et al. (2016); Birch et al. (2016); Tian et al. (2006); Zhu et al. (2019); Hsu et al. (2010); Dubey et al. (2018); Wang et al. (2019); Wang and Liu (2011); Krishnamurti et al. (2003), etc. They demonstrate that MJO can

Accepted for publication in *Journal of Climate*. DOI 10.1175/JCLI-D-23-0332.1.

interact with other processes over the tropic, such as typhoon and convection with a diurnal cycle. However, the role of multiscale interaction on the development of MJO has not reached a consensus. Scale-interactions are regarded as essential processes controlling MJO dynamics in some works (e.g., Majda and Biello 2003; Majda and Stechmann 2009). However, Zhou et al. (2012) propose that MJO gains its most energy from its own scale rather than other scales, and conclude that scale-interaction is not the dominant energy sources of MJO. Besides these disputes, it has also shown that the wind variabilities of MJO circumnavigate the globe (e.g., (Knutson and Weickmann 1987; Knutson et al. 1986; Ray and Li 2013)), but how the wind variabilities interact with other scale processes during its circumnavigating journey is still not clear. For all that account, we are hence motivated to deepen the understanding of MJO through diagnosing the multiscale energetics in a faithful and comprehensive way.

Multiscale energetics analysis has proved to be a powerful tool for multiscale interaction studies, ever since the pioneer work of Lorenz (1955). In this case, it however forms a challenging issue due to the propagating and evolving properties of MJO during its lifetime. Propagation means changing spatially, and evolution means changing temporally. In other words, MJO is localized in both space and time. Unfortunately, the traditional multiscale diagnosing methods are incapable in tackling localized problems (refer to section 2c for details). To overcome this problem, Liang et al. (2005; 2007; 2016) propose a localized multiscale energetics analysis methodology with the aid of a new mathematical apparatus — Multiscale Window Transform (MWT in short; refer to section 2c for details), on the basis of the theory of canonical transfer. This methodology is hence applied to analyzing the multiscale MJO dynamics henceforth.

The paper is organized as follows: Section 2 describes the datasets and methods as used. Reconstructed MJO signals are given in Section 3, and, correspondingly, the multiscale kinetic energy and available potential energy budgets are analyzed in Sections 4 and 5, respectively. Section 6 concludes the study and offers a discussion of some remaining issues.

2. Data and Method

a. Data

The ERA-Interim (Dee et al. 2011) dataset (including three-dimensional wind fields, geopotential, and temperature) is used in this study. We choose this dataset with a relatively

Accepted for publication in *Journal of Climate*. DOI 10.1175/JCLI-D-23-0332.1.

coarse resolution out of computing resources consideration. It has a temporal resolution of four times a day, and a spatial resolution of $3^{\circ} \times 3^{\circ}$. It spans the period from 05/28/1996, 0:00 through 10/31/2018, 18:00, making a series of 2^{15} time steps. Vertically it has 17 isobaric levels: 10, 20, 30, 50, 70, 100, 150, 200,225, 300, 400, 500, 600, 700, 850, 950, 1000 hPa, and horizontally it covers the zonal belt $39^{\circ}S - 39^{\circ}N$. The Outgoing Longwave Radiation (OLR) dataset from National Oceanic and Atmospheric Administration (Liebmann and Smith 1996) is used as a proxy for deep convection; it is on a daily basis and has a spatial resolution of $2.5^{\circ} \times 2.5^{\circ}$. Though we notice that there are different indices for tracking MJO (e.g., Kiladis et al. 2014; Wang et al. 2018), a daily RMM index (Wheeler and Hendon 2004) is used here to composite the MJO episodes by phase, considering that our focus is the large-scale variabilities of MJO in winter.

b. Multiscale window transform, multiscale energetics analysis, and canonical transfer

1) MULTISCALE WINDOW TRANSFORM

Multiscale window transform (MWT) is a newly developed functional apparatus (Liang and Anderson, 2007), which, while orthogonally making decomposition of a field by scale and providing filtered fields (reconstructions), also provides transform coefficients for the corresponding filtered fields. This not only ensures energy conservation during a decomposition, but also makes it possible to express multiscale energies in terms of transform coefficients. This is in contrast to most of the widely used filters, such as the Butterworth filter, which do not provide transform coefficients and hence cannot have this multiscale energy representation. (It is a common practice to use the square of filtered fields as multiscale energy, but that is conceptually wrong---think about the energy in Fourier space.)

In MWT, we reconstruct a field onto some range of scales, or *scale windows* as called. In this study, we will need a low-frequency window, an intraseasonal window, and a high-frequency window. For convenience, we will denote these windows as 0, 1, 2, respectively. An in-depth introduction of MWT is beyond this study. Here we simply write the MWT of a field, say *T*, as $\widehat{T}_n^{\sim\varpi}$, where *n* is the time step, $\varpi = 0,1,2$ denotes the scale window. The corresponding reconstructions, i.e., filtered fields, are written as $T_n^{\sim\varpi}$.

2) CANONICAL TRANSFER AND MULTISCALE ENERGETICS

Accepted for publication in *Journal of Climate*. DOI 10.1175/JCLI-D-23-0332.1.

Multiscale energetics analysis has become a powerful tool to diagnose the dynamical processes underlying atmospheric phenomena ever since Lorenz's seminal work (1955). However, Lorenz's formalism is in a bulk form, lacking the needed local information for most of the weather and climate processes, particularly for those moving and developing processes. Numerous studies seek to circumvent this limitation by simply removing the average operators. This seems to be effective in practice, but is wrong. As elaborated in Liang (2016) and many publications, a most recent one being Yang et al. (2020), that removing the average operator from the eddy energy formula with a Reynolds decomposition does not yield the "localized eddy energy"; in fact, it is not energy at all. The average operator allows for a connection of the so-obtained eddy energy to the eddy energy in the Fourier space through Parseval relation. Second, localizing the bulk Lorenz formalism is faced with an obstacle on how to separate the cross-scale transfer from in-scale transport, which is rather subjective in classical formalisms and not unique. This is a rather fundamental problem (e.g., Plumb 1983) which, however, has been mostly overlooked. Liang and Robinson (2005, 2007) is the first to tackle this systematically, using the aforementioned MWT as the machinery. The thus-obtained transfer proves to be unique later on Liang (2016), and bears a Lie bracket form, satisfying the Jacobian identity, among many other properties. They hence call it *canonical transfer*. As here it is not our focus, we just give a simple introduction of the formula for computation. For a a scalar field T in an incompressible flow $\mathbf{v}$, the canonical transfer to window ϖ at time step n is

$$\Gamma_n^{\varpi} = -E_n^{\varpi} \nabla \cdot \left[\frac{\widehat{(\mathbf{v}T)}_n^{\sim\varpi}}{\widehat{T}_n^{\sim\varpi}} \right],$$

where E_n^{ϖ} is the energy on window ϖ at time step n. This transfer has a nice property $\sum_{\varpi}\sum_{n}\Gamma_n^{\varpi} = 0$, which means that this kind of process only redistributes energy among scales; it does not generate nor destroy energy as a whole; in other words, it ensures energy conservation, in contrast to the traditional counterparts.

With the machinery MWT and the theory of canonical transfer, the localized multiscale energetics analysis is made possible. In the following we just give a symbolic expression for the multiscale kinetic energy and available potential energy equation [see (Liang 2016) for derivation], which we will use for the purpose of this study:

Accepted for publication in *Journal of Climate*. DOI 10.1175/JCLI-D-23-0332.1.

$$\frac{\partial K^{\varpi}}{\partial t}+\underbrace{\nabla\bullet\left[\frac{1}{2}(\mathbf{v}\mathbf{v}_h)^{\sim\varpi}\bullet\mathbf{v}_h^{\sim\varpi}\right]}_{\nabla\bullet\mathbf{Q}_K^{\varpi}}=\underbrace{\frac{1}{2}\left\{(\mathbf{v}\mathbf{v}_h)^{\sim\varpi}:\nabla\hat{\mathbf{v}}_h^{\sim\varpi}-\left[\nabla\bullet(\mathbf{v}\mathbf{v}_h)^{\sim\varpi}\right]\bullet\hat{\mathbf{v}}_h^{\sim\varpi}\right\}}_{\Gamma_K^{\varpi}}$$
$$-\underbrace{\nabla\bullet\left(\hat{\mathbf{v}}^{\sim\varpi}\hat{\Phi}^{\sim\varpi}\right)}_{\nabla\bullet\mathbf{Q}_P^{\varpi}}-\underbrace{\hat{\omega}^{\sim\varpi}\hat{\alpha}^{\sim\varpi}}_{b^{\varpi}}+R_K \tag{1}$$

$$\frac{\partial A^{\varpi}}{\partial t}+\underbrace{\nabla\bullet\left[\frac{1}{2}c(\mathbf{v}T)^{\sim\varpi}T^{\sim\varpi}\right]}_{\nabla\bullet\mathbf{Q}_A^{\varpi}}=\underbrace{\frac{c}{2}\left[\left(\mathbf{v}T\right)^{\sim\varpi}\bullet\nabla T^{\sim\varpi}-T^{\sim\varpi}\nabla\bullet\left(\mathbf{v}T\right)^{\sim\varpi}\right]}_{\Gamma_A^{\varpi}}$$
$$+\underbrace{\hat{\omega}^{\sim\varpi}\hat{\alpha}^{\sim\varpi}}_{b^{\varpi}}+R_A \tag{2}$$

where K^{ϖ} and A^{ϖ} is kinetic energy (KE) and available potential energy (APE) on window ϖ, and T is temperature, Φ geopotential, $\mathbf{v}$ velocity field, and $\mathbf{v}_h$ its horizontal component, Q_K KE transport, Q_A APE transport, Γ_K canonical KE transfer, Γ_A canonical APE transfer, Q_P work done by pressure gradient force, and *b* buoyancy conversion. R_K and R_A are the residues in the KE and APE balances, representing the other processes (including the work done by external forcings and energy sinks due to dissipation/diffusion). The colon operator ‘‘:’’ is defined such that, for two dyadic products $\mathbf{AB}$ and $\mathbf{CD}$, $(\mathbf{AB}):(\mathbf{CD})=(\mathbf{A}\cdot\mathbf{B})(\mathbf{C}\cdot\mathbf{D})$. Note for simplicity, the dependence on the time step n has been suppressed. Liang and Robinson (2007) establish that a positive canonical transfer from window 0 to window 1 correspond precisely to a barotropic instability of the basic flow.

MWT and the MWT-based multiscale energetics analysis have been applied with success to many different atmosphere-ocean-climate problems. The most recent ones include storm track (Zhao et al. 2019), atmospheric blocking (Ma and Liang 2017, 2023a), cold wave outbreak (Xu and Liang 2020), North Atlantic Oscillation (Ma and Liang 2023b), Gulf of Mexico circulation (Yang et al. 2020), to name a few.

3) COMPOSITE PROCEDURES

Variables are averaged to obtain their respective composites if the following two criteria are met: 1) amplitudes of their corresponding RMM indices are greater than one; 2) the RMM indices are in the same phase. For the energetics composition, the multiscale energy budget terms among three scale windows, namely, high-frequency window, intraseasonal window and low-frequency window, are calculated firstly, and then the compositing is conducted.

Accepted for publication in *Journal of Climate*. DOI 10.1175/JCLI-D-23-0332.1.

3. Scale separation and reconstructed composite MJO signal

To composite MJO, two steps are conducted successively. Firstly, the original fields are transformed through MWT with respect to an orthogonal basis, and then reconstructed onto three scale windows, namely, high-frequency window (shorter than 32 days), intraseasonal window (32-128 days) and low-frequency window (longer than 128 days). Next, variables on the intraseasonal window are composited (refer to Section 2 for composite procedures). Previous studies (e.g., Wang and Rui 1990; Zhang and Dong 2004) show that MJO experiences an obvious seasonal variation and its characteristics during summer and winter are different, so only the MJO episodes occurring from November to April are included in the composition here.

The composite MJO has been well characterized in previous studies (e.g., Hendon and Salby 1994; Maloney and Hartmann 1998; Kiladis et al. 2005; Adames and Wallace 2014a, 2015, 2014b); here we only take a glance at the composite temperature and zonal wind fields on the intraseasonal window (Fig. 1), as these fields determine the two types of the energy — the available potential energy and kinetic energy, which form the focus of this study. Figs. 1-2 depict, respectively, the meridionally averaged (from $10^{\circ}S$ to $10^{\circ}N$) zonal-vertical sectional distribution of the composite MJO temperature and zonal wind fields. OLR are added here to denote the location of deep convection as associated. From Figs.1 and 2, obvious temperature and zonal wind anomalies accompanying the convection anomalies, which propagate eastward slowly, are found during the MJO lifetime. Loosely speaking, the temperature and convection anomalies are almost in phase, while the zonal wind is in quadrature phase with the convection anomalies.

In detail, temperature anomalies mainly occur above 400 hPa through 150 hPa. In this layer, positive (negative) temperature anomalies accompany positive (negative) convection anomalies until the convection hits the dateline, when convections decay gradually. For the zonal wind anomalies, the positive convection anomalies lag the easterlies but lead the westerlies in the upper level. In the low level, this relation reverses—the positive convection anomalies lead the easterlies but lag the easterlies. These wind anomaly structures reflect the convergences in low level and divergence in upper level within the convection regions. The layout of the divergence in the upper over the convergence in the lower matches well the maximum upperward motion in the middle level. This has been well recognized since Madden and Julian (1972), and is one of the core issues in understanding MJO. It is closely

Accepted for publication in *Journal of Climate*. DOI 10.1175/JCLI-D-23-0332.1.

connected with large-scale circulation and convective processes. Hence, understanding the interaction between large-scale circulation and convective processes is one of the major tasks in the studies of MJO dynamics. Essentially, the interaction between the convections and circulation forms a particular case of multiscale interaction, which we will study in the next section in terms of multiscale energetics. After the eastern edge of the convection reaches the dateline, it terminates and decays gradually. However, the accompanied zonal wind anomalies continue to propagate across the dateline, and even get re-strengthened over $90^{\circ}\mathrm{W}$. By examining the extent of the zonal wind, we find that they travel around the whole globe after crossing the dateline in the upper level, but almost disappear in the low level in the Western Hemisphere. The variations in propagating speed are also found in Fig. 2 here. For example, from Phase 3 to Phase 6, the easterlies propagate from $60^{\circ}\mathrm{E}$ to almost $150^{\circ}\mathrm{E}$, but its counterpart westerlies propagate from $180^{\circ}\mathrm{E}$ thorough the whole western hemisphere and reach Indian Ocean (almost $60^{\circ}\mathrm{E}$) over the same period in the upper level. In other words, the travelling distance is beyond twice longer over the western hemisphere than eastern hemisphere within the same time.

The Hovmöller diagram of the reconstructed OLR signals on the intraseasonal window through 1997 (Fig. 3) is plotted to verify the filtering process. Evident MJO episodes are found from January through June in the year. Clearly shown is a prominent feature of the slowly eastward propagation. The OLR anomalies are also found to develop over the Indian Ocean and decay east of the dateline. Based on these facts, we can safely conclude that the reconstructed signals on the intraseasonal window have well captured the main characteristics of MJO.

To summarize, though different composite and filtering methods are used in this paper, consistent MJO characteristics are reproduced with previous studies (e.g., Hendon and Salby, 1994). In the following we therefore study the mechanisms controlling the evolutions of these characteristics.

Accepted for publication in *Journal of Climate*. DOI 10.1175/JCLI-D-23-0332.1.

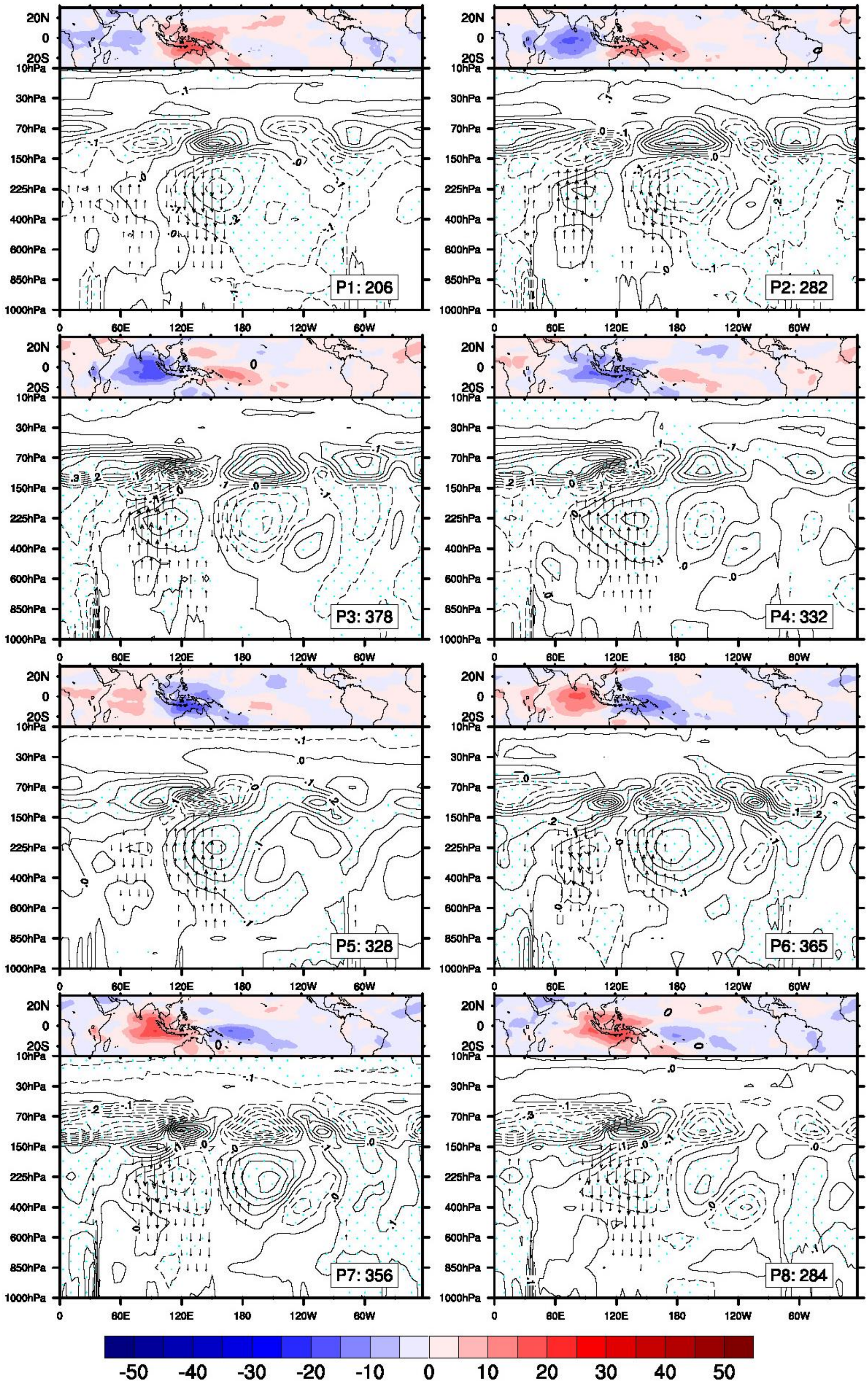

Accepted for publication in *Journal of Climate*. DOI 10.1175/JCLI-D-23-0332.1.

Fig. 1 Zonal-vertical sectional distribution of the temperature (^oK, contoured) and vertical velocity (Pa/s, vectors) averaged over $10^{\circ}S-10^{\circ}N$ and outgoing longwave radiation (W/m^2, shaded) on the intraseasonal window from Phase 1 to Phase 8. “P” in the bottom right boxes means “Phase” and the numbers in the box mean the numbers of days in each phase involved in the composition. Dotted are the regions of temperature statistically significant at the 95% level by the Student’s *t* test.

Accepted for publication in *Journal of Climate*. DOI 10.1175/JCLI-D-23-0332.1.

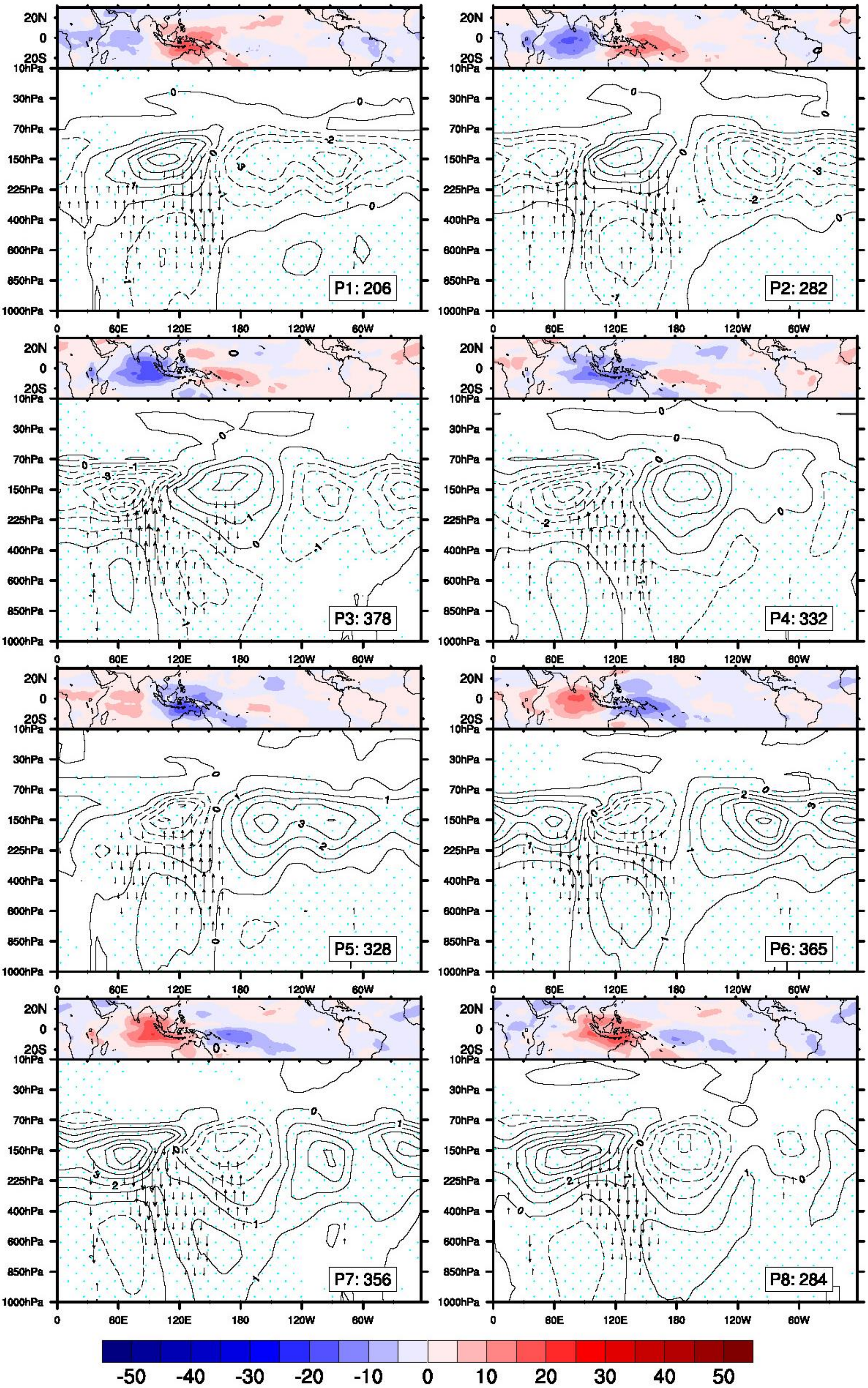

Accepted for publication in *Journal of Climate*. DOI 10.1175/JCLI-D-23-0332.1.

Fig. 2 Zonal-vertical sectional distribution of the zonal velocity (m/s, contoured) and vertical velocity (Pa/s, vectors) averaged over $10^{\circ}S-10^{\circ}N$ and outgoing longwave radiation (W/m^2, shaded) on the intraseasonal window from Phase 1 to Phase 8. "P" in the bottom right boxes means "Phase" and the numbers in the box mean the numbers of days in each phase involved in the composition. Dotted are the regions of zonal velocity statistically significant at the 95% level by the Student's *t* test.

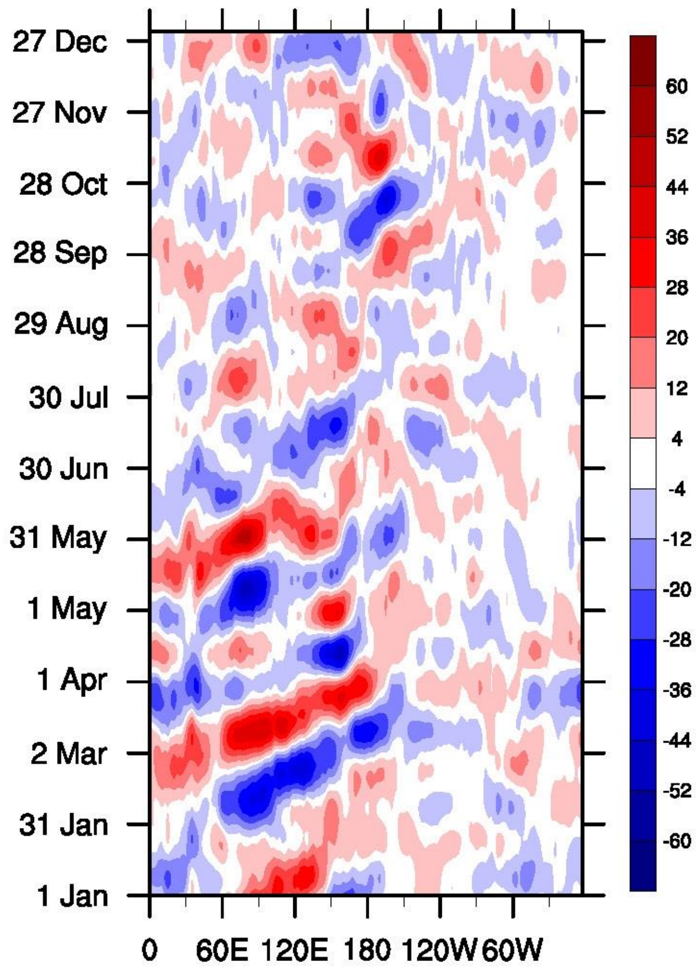

Fig. 3 Hovmöller diagram of the reconstructed OLR signals on the intraseasonal window through 1997 (units: W/m^2).

4. Multiscale dynamics

a. Phase selection

Accepted for publication in *Journal of Climate*. DOI 10.1175/JCLI-D-23-0332.1.

By previous studies the wind variabilities of MJO in the upper troposphere has a planetary scale and a zonal wavenumber-1 structure. However, we find that the zonal extent of their westerlies and easterlies (Fig. 4) is actually time-dependent. In Phases 4 and 8, their zonal extents are almost the same, both covering half of the equator. In contrast, in Phases 2 (resp. 6), the easterlies (westerlies) zonal extent is almost three times of westerlies (resp. easterlies) zonal extent. The extents in other phases are in between. Using the contrast between the easterlies and westerlies extents as a criterion, we pick two groups out of the 8 phases of MJO to analyze their dynamics. Group 1 has the minimum contrast, and consists of phases 2 and 6, while group 2 has the maximum of that, including phases 4 and 8. Though there are two opposite phases in each group, the dynamics underlying the two phases in the same group are essentially the same (not shown). We henceforth only need to choose phases 2 and 4 in investigating the underlying dynamics.

Accepted for publication in *Journal of Climate*. DOI 10.1175/JCLI-D-23-0332.1.

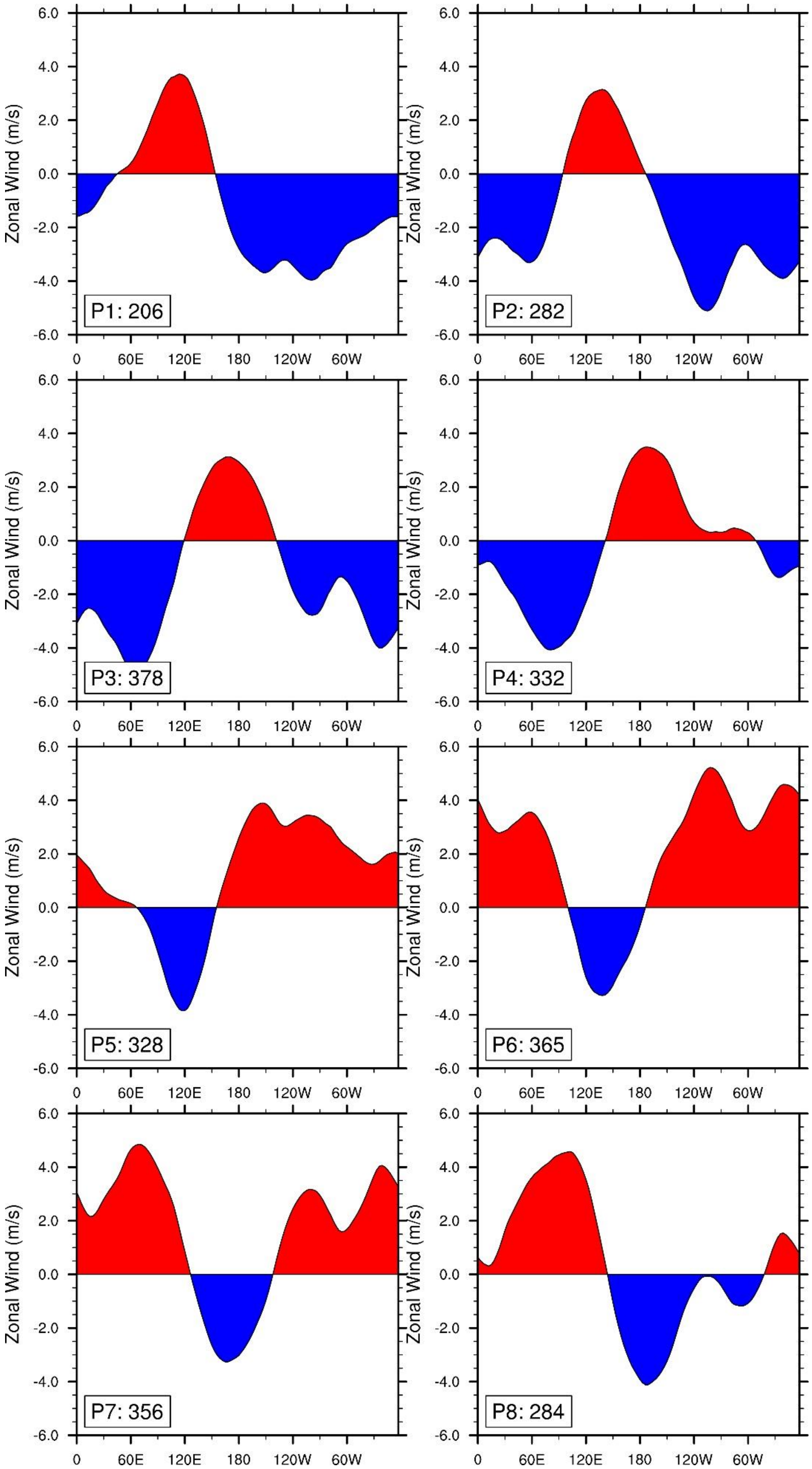

Accepted for publication in *Journal of Climate*. DOI 10.1175/JCLI-D-23-0332.1.

Fig. 4. The means of the wind variabilities at 150 hPa and 100hPa on the intraseasonal window averaged over $10^{\circ}\mathrm{S}-10^{\circ}\mathrm{N}$ from Phase 1 to Phase 8. The “P” in the bottom-left box of a subplot means the phase, and the number means the number of days in that phase involved for composition.

A well-known characteristic of the MJO wind variability is that the propagation speed is much faster over the Western Hemisphere than that over the Eastern Hemisphere. HS94 proposed that the mechanisms underlying this contrast is that the variability of MJO is a Rossby-Kelvin wave mingled with convections over the Eastern Hemisphere, while over the Western Hemisphere it is a radiated Kelvin wave. We claim that phase 4 here provides a reasonable framework for the study of the dynamics of MJO variabilities superimposed with convections over the Eastern Hemisphere. Here it is why: Firstly, the convection over the Eastern Hemisphere is well-developed and in quadrature with the wind fields, so the wind variabilities are strongly modulated by the convection. Secondly, the KE of the variability is almost confined over the Eastern Hemisphere and Eastern Pacific ($0°\mathrm{E} - 120°\mathrm{W}$), and does not spread into other regions of the Western Hemisphere (especially in the region $120°\mathrm{W} - 0°\mathrm{W}$). Another evidence supporting the close relationship between phase 4 here and MJO variabilities superimposed with convection is that it is similar to the most unstable mode of the “frictional wave-CISK” simulation of Wang and Rui (1990) and Salby et al. (1994). Also, we find that phase 2 could reveal the dynamics of the radiated fast-moving variabilities of MJO. This is supported by two facts. (1) The KE extends to everywhere over the Western Hemisphere; that is to say, it occupies over all the zonal tropic belt. (2) The wavelength of the wind anomalies over the Western Hemisphere is much longer than their Eastern Hemisphere counterparts, manifesting a higher speed of propagation over the Western Hemisphere.

Understanding the interaction between the circulation and the convection is essential to understand the MJO dynamics. Two well-recognized interactive performances of convection and circulation are that wind variabilities are radiated to western hemisphere quickly after the convection terminates east of the dateline (e.g., Hendon and Salby 1994), while the wind variabilities in turn affect the convection initiation after they cross the western hemisphere and reach the Africa-India Ocean region(e.g., Ray et al. 2011; Roundy 2014; Sakaeda and Roundy 2015). Hence, understanding the multiscale dynamics of MJO is important. To do so,

Accepted for publication in *Journal of Climate*. DOI 10.1175/JCLI-D-23-0332.1.

we proceed to analyze the multiscale kinetic and available potential energetics of MJO during phases 2 and 4, respectively.

In a word, these two phases represent two essential elements of the MJO dynamics, with one related to the convection-coupled dynamics and the other to the radiated dynamics. We hence will concentrate on the multiscale dynamics underlying these two phases in this paper.

b. On the multiscale KE budget

1) PHASE 4

For phase 4, the wind anomalies, and hence the KE, have two dominant centers — one over $30\text{-}120^{\circ}\mathrm{E}$ and the other $150\text{-}210^{\circ}\mathrm{E}$ in the upper layer (contours, P4 and P8 in Fig. 2). These two centers will be referred to as the western center and the eastern center hereafter. Examining Figs. 5, we find that the KE of the western center mainly comes from the canonical KE transfer from the low-frequency window to intraseasonal window, while the eastern one gains its KE mostly from the upper layer through pressure work. Phase 4 reflects the circulations in the existence of the deep convection forcing over the Eastern Hemisphere, reminding us the well-known Gill model. In Gill's theory, Kelvin waves dominate at the east of the convection, while Rossby waves dominate at the western side. As we know, Kelvin wave is a kind of gravity wave and pressure works are hence supposed to play an important role in its development. Our findings about the eastern center is consistent with this. However, the canonical KE transfer gain from the low-frequency window at the western center and loss to the low-frequency window at the eastern center tell us that the western center is not free Kelvin wave or Rossby wave mode as described in the Gill model, but forced by the low-frequency processes. The new finding here is that phase 4 is not only forced by the convection, but also by the background flow. KE transports are sinks of KE for the two centers, while buoyancy conversion contributes KE to them in the lower layer of the centers but consumes KE in their upper layer. KE transfer from the high-frequency window to the intraseasonal window is almost negative everywhere but with much smaller magnitudes than the other processes. In the lower layer, dominantly the KE is gained via pressure work, consistent with Zhou et al. (2012). The residual processes mainly take place over the regions where convective processes exist, making a KE source for the western center.

Accepted for publication in *Journal of Climate*. DOI 10.1175/JCLI-D-23-0332.1.

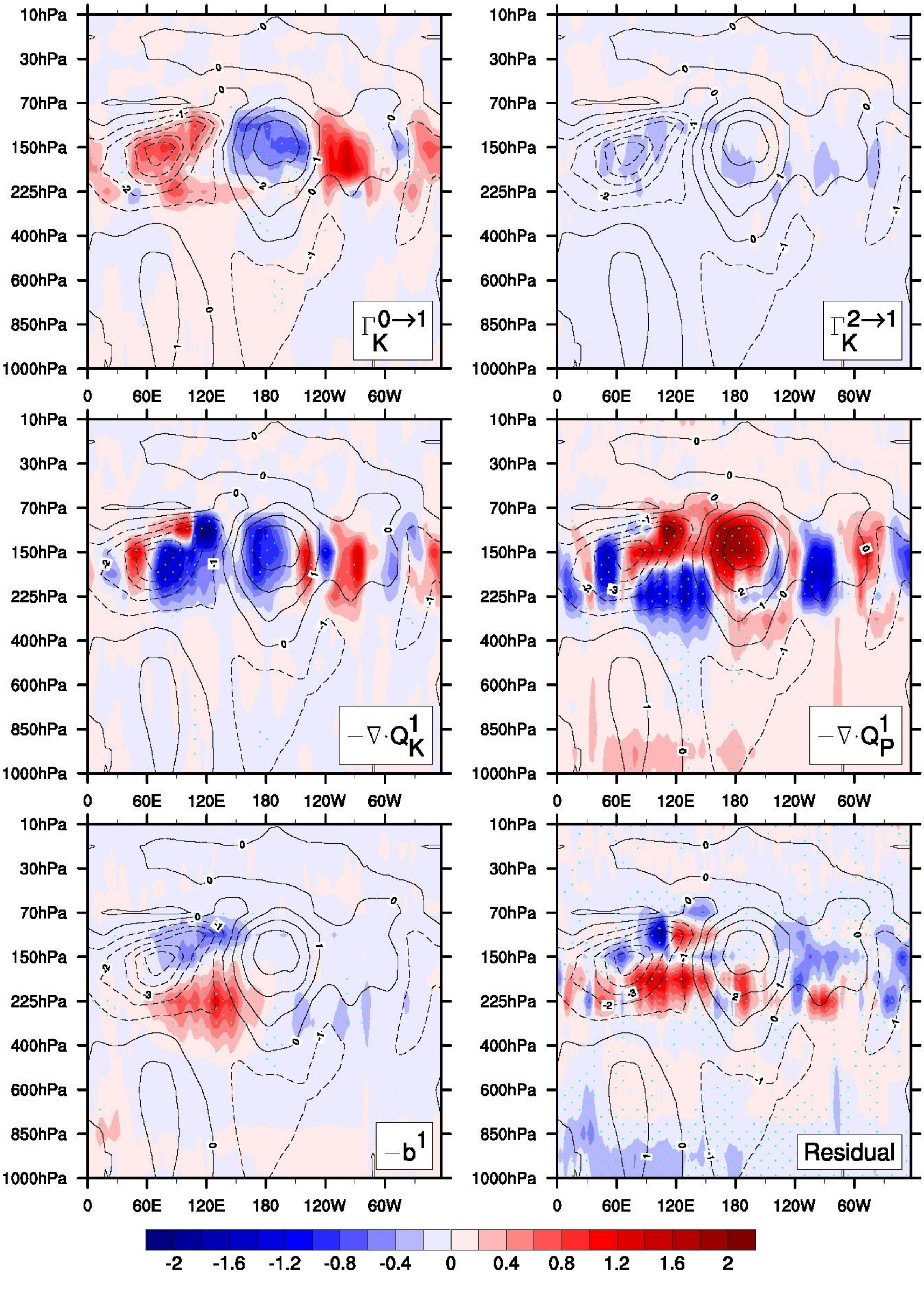

File generated with AMS Word template 2.0

Accepted for publication in *Journal of Climate*. DOI 10.1175/JCLI-D-23-0332.1.

Fig.5 The canonical KE transfer from the low-frequency window to the intraseasonal window ($\Gamma_K^{0\to1}$, in $10^{-4}m^2s^{-3}$, shaded; same below), and that from the high-frequency window to the intraseasonal window ($\Gamma_K^{2\to1}$, in $10^{-4}m^2s^{-3}$), the KE transport ($-\nabla\cdot Q_K^1$, in$10^{-4}m^2s^{-3}$), work done by pressure ($-\nabla\cdot Q_P^1$, in $10^{-4}m^2s^{-3}$), buoyancy conversion ($-\mathrm{b}^1$, in $10^{-4}m^2s^{-3}$) on the intraseasonal window, and the residual of the energetics (residual, in $10^{-4}m^2s^{-3}$). Contoured is the zonal-vertical sectional distribution of the zonal velocity (m/s) on the intraseasonal window. All the variables are averaged over $10^\circ\mathrm{S}-10^\circ\mathrm{N}$ during phase 4. Dotted are the regions statistically significant at the 95% level by the Student's *t* test.

2) PHASE 2

A sharp contrast between the westerly and easterly wavelengths is found in phase 2. For example, in Fig. 2, the easterlies span from $180^\circ\mathrm{E}$ to $90^\circ\mathrm{E}$ (270°), but the westerlies span from $90^\circ\mathrm{E}$ to $180^\circ\mathrm{E}$ (90°) in the upper (lower) layer during Phase 2 --- the wavelength of the former is almost three times the latter. Distinct from phase 4, phase 2 has four KE centers in the upper layer. For easy reference, they are hereafter referred to as, from west to east by location, India-Ocean center, Western-Pacific center, Eastern-Pacific center and Atlantic center, respectively. However, only the Western-Pacific center in the upper layer has a counterpart KE center in the lower layer. This is a manifest of weaker coupling of zonal winds between the upper and lower layers at centers other than the Western-Pacific center. Further investigation shows that the Western-Pacific center has dynamical processes completely different from the other three (Fig. 6). The main KE sources of the Western-Pacific center and its counterpart in the low layer are both pressure work. However, dominant KE sources of the other centers are the canonical KE transfer from the low-frequency window to the MJO window. (Note that, though the magnitudes of pressure work and KE transport at the other three centers are large, they are mostly offset, hence cancelled out, by each other.) An interesting observation is that there exists evident difference between the KE transport processes of MJO over the Eastern Hemisphere and the Western Hemisphere. To be specific, the Western-Pacific center and India-Ocean center over the Eastern Hemisphere are sinks of KE, similar to that in phase 4, while they show up with dipolar patterns at the other two centers over the Western Hemisphere. For the latter, it is found that KE is transported

Accepted for publication in *Journal of Climate*. DOI 10.1175/JCLI-D-23-0332.1.

from the western halves of the centers to their respective eastern halves, facilitating the eastward propagation of MJO. These characteristics of KE transport seems to partly account for the faster propagation over the Western Hemisphere than over the Eastern Hemisphere. These findings confirm the early statement, which we made in section 4a, that phase 2 can reveal the radiated dynamics of MJO. Similar to phase 4, buoyancy conversions are KE sources for the centers over the Eastern Hemisphere in their lower layer but sinks in their upper layer, but over the Western Hemisphere, there are no evident buoyancy conversions near the centers in phase 2. Besides, the KE transfer from the high-frequency window to the intraseasonal window is almost negative everywhere, albeit negligible on the whole. For the residual, it essentially functions as a KE source and sink over the Eastern Hemisphere and Western Hemisphere, respectively.

In previous studies, it is believed that the intraseasonal variabilities over the Western Hemisphere are Kelvin waves radiated from the terminated convection near the dateline (e.g., Hendon and Salby, 1994; 1996). However, Roundy (2014) find that the intraseasonal wind variabilities become stronger over $90^{\circ}\mathrm{W}$ after it separates from the convection. Similar phenomenon has been observed in our composite in phase 2. This demonstrates that the radiated energy from the convection is definitely not the only energy source for the wind variabilities over the Western Hemisphere. Advection of convergent background wind by intraseasonal winds and equatorward intrusion of extratropical waves are regarded as extra energy sources in previous works (Roundy 2014; Sakaeda and Roundy 2015). Our budget of multiscale energetics shows that the canonical KE transfer from low-frequency window accounts for it. This mean the wind variabilities of MJO over the Western Hemisphere can not be simply regarded as free dry or moist Kelvin waves, as in the previous studies (e.g., Hendon and Salby 1994; Matthews 2000; Sobel and Kim 2012; Roundy 2012). Our results here show that the radiated energy from the convection over the Eastern Hemisphere is not the only source of the MJO wind variabilities over the Western Hemisphere; barotropic instability provides a substantial part of energy for their maintenance.

Another interesting observation is the contrast distribution of canonical KE transfer over the eastern and western Pacific for phases 2 and 4. More specifically, MJO loses KE to the low-frequency window over the western Pacific, while gaining energy from the low-frequency window over the eastern Pacific (Figs. 5 and 6). Analyzing this special distribution, we can find that the low-frequency variabilities behave like a “bridge” which

Accepted for publication in *Journal of Climate*. DOI 10.1175/JCLI-D-23-0332.1.

helps the MJO signal cross the Pacific. In other words, MJO stores its energy, which it gains from the work done by the pressure gradient force, into the low-frequency window over the western Pacific, and then the low-frequency window releases the part of energy back to the intraseasonal window over the eastern Pacific. In fact, how the MJO propagates across Pacific is still a controversial issue (e.g., Hsu and Lee, 2005), and here we find another plausible mechanism.

Accepted for publication in *Journal of Climate*. DOI 10.1175/JCLI-D-23-0332.1.

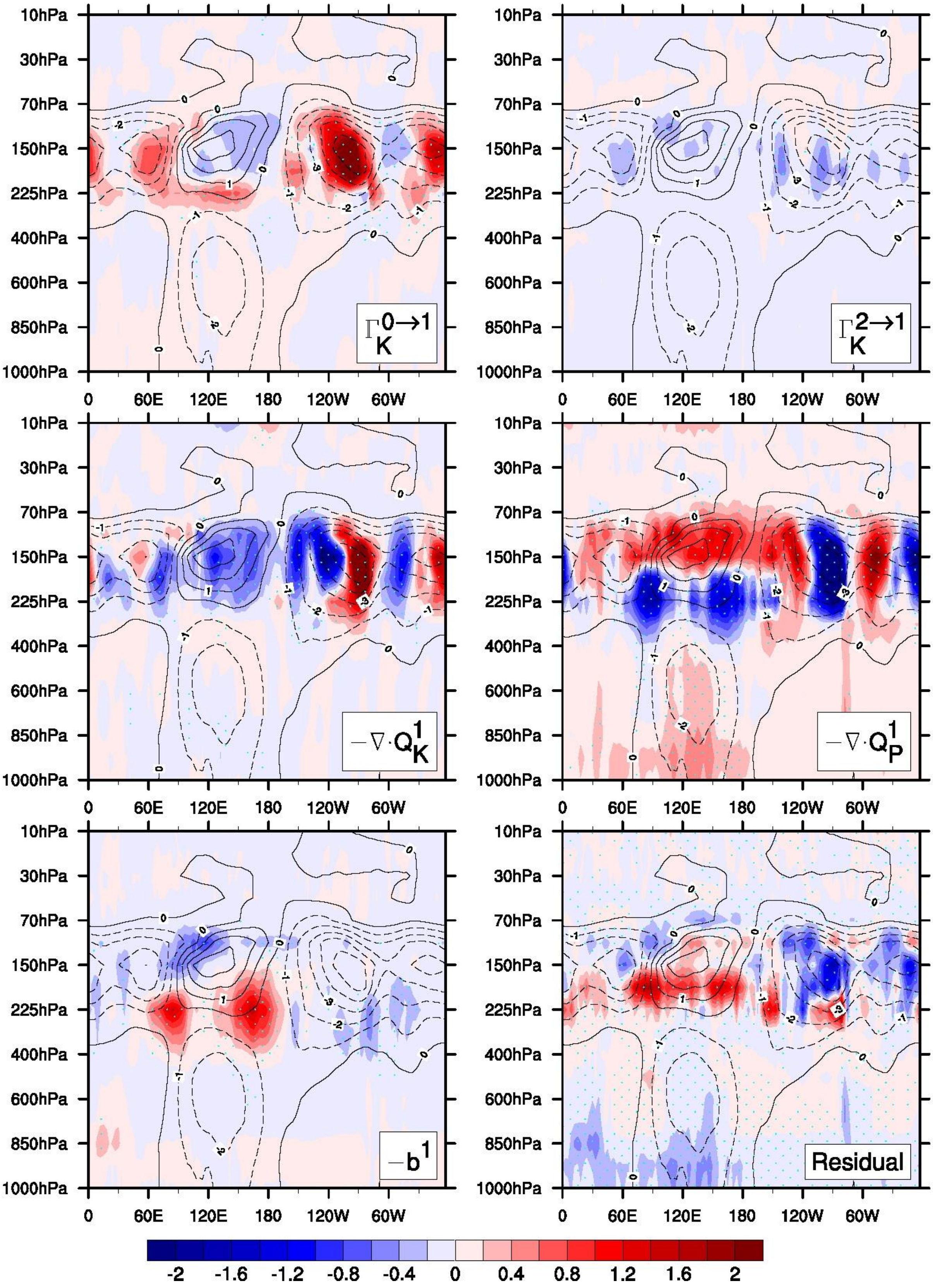

Fig.6 As in Fig. 5, except that the budget is for phase 2.

Accepted for publication in *Journal of Climate*. DOI 10.1175/JCLI-D-23-0332.1.

c. On the multiscale APE budget

Budgets of APE are conducted to explain the existence of the thermodynamics of MJO (Figs. 7-8). It should be pointed out that the conversion between available potential energy and kinetic energy in Fig. 5 is precisely opposite in sign to that in Fig. 7, as well as that in Fig. 6 to Fig. 8. (Note that they have different colorbars.) Phases 4 and 2 are discussed as a whole since they have similar behaviors. An intriguing finding from the spatial distribution is that the dominant energetic processes only occur over $60\text{-}180^{\circ}\mathrm{E}$, becoming insignificant elsewhere (Figs. 7-8). This is the region where most of the deep convection occurs, implying that the thermodynamic processes are closely related to the convection. Another evidence supporting this statement is that all the thermodynamic processes are closely related with the vertical motion as shown by the vectors in Figs.7-8. There is only an upward motion in phase 4, but an upward and a downward motion in phase 2. Correspondingly, all the thermodynamic processes concentrate near the upward motion region in phase 4, while in phase 2 they are split into two regions, one occupying the upward motion region and the other occupying the downward motion region.

The most obvious temperature anomalies of MJO show up from 500 hPa through 200 hPa. In this layer, the sources of the available potential energy on the MJO window include APE transport and canonical APE transfer from low-frequency scale to intraseasonal scale, and buoyancy conversion is its sink. Canonical APE transfer from high-frequency scale to intraseasonal scale is negligible in this composite budget. Particularly, APE transport process has APE transported from the surrounding regions to convective region. In this sense, APE transport on the MJO window facilitates the convective organization of MJO. Similar to APE transport, the canonical APE transfer from the low-frequency scale to intraseasonal scale also contributes to the development of the temperature anomalies of MJO. For the residual, an obvious feature is that there is a critical level near 300 hPa separating its positive and negative contributions to APE generation. It is an APE source underneath this level but a sink above. Hagos et al. (2011) propose that the dominant APE source is convective latent heating, but our analysis here indicates that not only this external forcing, but also the internal atmospheric processes, are important in producing the APE needed for MJO. These results illustrate that the temperature anomalies of MJO should not be simply understood as a response to convective heating. Its formations involve complex dynamical processes.

Accepted for publication in *Journal of Climate*. DOI 10.1175/JCLI-D-23-0332.1.

Another well-known feature of the MJO temperature anomalies is the tilting eastward with height near the tropopause over the convective regions (e.g., Kiladis et al. 2005), which is believed to be caused by the adiabatic lofting forced by the convective processes below (Sherwood et al. 2003), and is related to the upward propagating gravity wave response to eastward moving MJO convective forcing (Kiladis et al. 2005). By diagnosing the APE budget here, we find that these anomalies are controlled by buoyancy conversion and canonical APE transfer from MJO to the low-frequency window. Buoyancy conversion is its APE source, while the canonical APE transfer from MJO to the low-frequency window makes a sink.

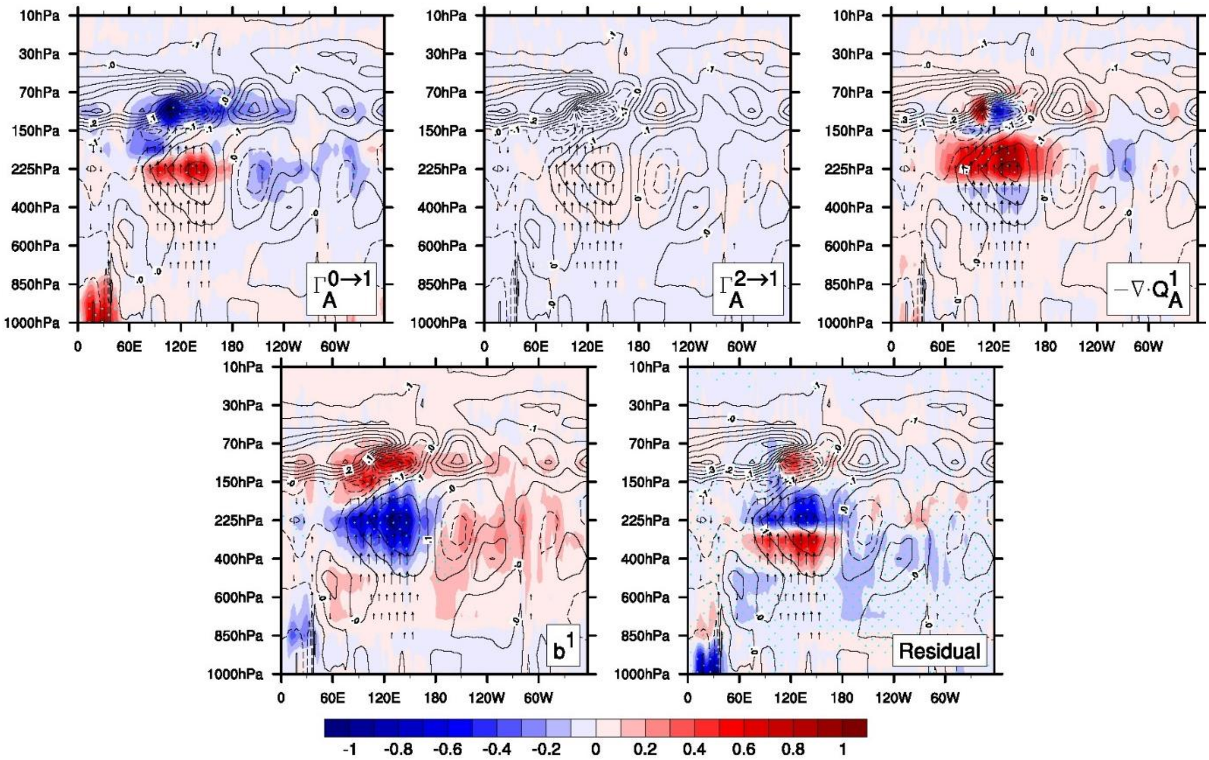

Fig. 7. The canonical APE transfer from the low-frequency window to the intraseasonal window ($\Gamma_A^{0\to1}$, in $10^{-4}m^2s^{-3}$, shaded; same below), and that from the high-frequency window to the intraseasonal window ($\Gamma_A^{2\to1}$, in $10^{-4}m^2s^{-3}$), the APE transport ($-\nabla\cdot Q_A^1$, in $10^{-4}m^2s^{-3}$), buoyancy conversion (b^1, in $10^{-4}m^2s^{-3}$) on the intraseasonal window, and the residual of the energetics (residual, in $10^{-4}m^2s^{-3}$). Contoured is that zonal-vertical sectional distribution of the temperature ($^\circ K$) on the intraseasonal window. The vectors are vertical velocity, which are used to denote the location of the convection anomalies. All the variables are averaged

File generated with AMS Word template 2.0

Accepted for publication in *Journal of Climate*. DOI 10.1175/JCLI-D-23-0332.1.

over $10^{\circ}\mathrm{S}-10^{\circ}\mathrm{N}$ during phase 4. Dotted are the regions statistically significant at the 95% level by the Student's *t* test.

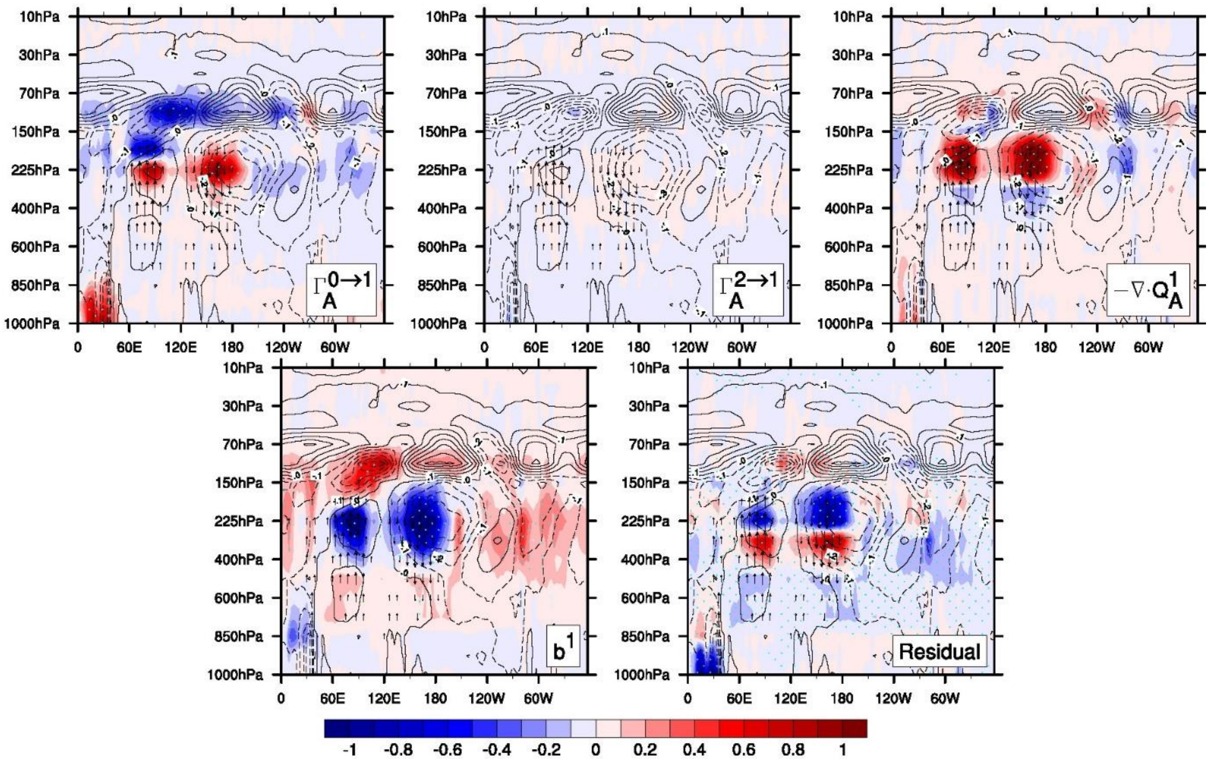

Fig. 8. As in Fig. 7, except that the budget is for phase 2.

5. Dynamical contrast of MJO over the Eastern and Western Hemispheres

It is well known that MJO has distinct features over the Eastern and Western Hemispheres. In its course from the Eastern Hemisphere to the Western Hemisphere, a prominent transition is that its convective processes get weaker or even vanish after crossing Eastern Pacific, and then its wind variabilities travel much faster over the Western Hemisphere than that over the Eastern Hemisphere (Knutson and Weickmann 1987; Hendon and Salby 1994). Based on this fact, a contrast in dynamics for the MJO variabilities over the Eastern and Western Hemispheres is hence naturally anticipated. Multiscale energy budgets are thus studied to show the contrast. From Fig. 4, the kinetic energy (KE) of the MJO wind variabilities has the smallest extent and is almost confined to the Eastern Hemisphere and Eastern Pacific (0°E – 120°W), while it is relatively weak and negligible over most region of the Western Hemisphere (120°W – 0°W) in Phase 4. In other words, MJO wind anomalies over the Eastern and Western Hemispheres are in sharp contrast in this phase; no comparison

Accepted for publication in *Journal of Climate*. DOI 10.1175/JCLI-D-23-0332.1.

of dynamics will be meaningful since one is essentially negligible. We hence focus only on Phase 2, in which the wind anomalies are comparable over the whole tropic.

The budgets of KE as shown in Fig. 9 tell that the dominant terms for the Eastern Hemisphere are pressure work, KE transport, and canonical KE transfer, while for the Western Hemisphere the cross-scale canonical KE transfer, buoyancy conversion and residual term dominate. By this over the Eastern and Western Hemisphere the MJO dynamics are evidently different. For energy sources, pressure work is dominant and canonical KE transfer from the low-frequency window to MJO is secondary over the Eastern Hemisphere, while the latter dominates over the Western Hemisphere. For energy sinks, the dominant processes are KE transport over the Eastern Hemisphere but buoyancy conversion and residual processes dominate over the Western Hemisphere. In contrast to the drastic change of the canonical KE transfer from the low-frequency window to MJO over the Eastern and Western Hemisphere, the canonical KE transfer from the high-frequency window rarely varies --- it always extracts KE from MJO to fuel the convections over both Hemispheres.

As regard to the role of multiscale interaction in the MJO maintenance and propagation, by above we can safely say that the canonical KE transfer from the low-frequency window to MJO facilitates the maintenance of MJO variabilities, especially over the Western Hemisphere.

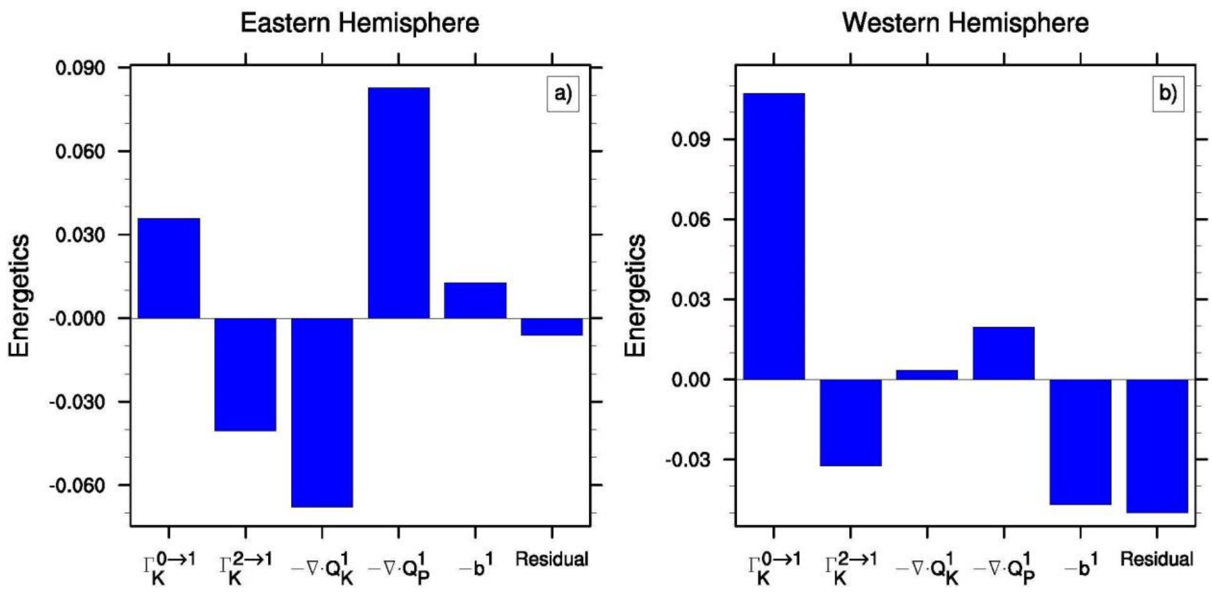

Fig. 9 Kinetic energetics averaged over (a) the Eastern Hemisphere $[0° - 180°\mathrm{E}, 10°\mathrm{S} - 10°\mathrm{N}]$ and (b) the Western Hemisphere $[0° - 180°\mathrm{W}, 10°\mathrm{S} - 10°\mathrm{N}]$ and

Accepted for publication in *Journal of Climate*. DOI 10.1175/JCLI-D-23-0332.1.

throughout the vertical levels (1000hPa-100hPa) in RMM Phase 2. Refer to Fig. 5 for the meaning of the symbols.

6. Conclusion and discussion

A newly developed functional analysis apparatus, multiscale window transfer (MWT) and the MWT-based methodology for multiscale energetics analysis have been employed to study the maintenance and propagation of MJO. We first reconstructed the original field variables onto three scale windows, namely, high-frequency window (shorter than 32 days), intraseasonal scale window (32-128 days) and low-frequency window (longer than 128 days). Through compositing the reconstructed/filtered variables on the intraseasonal scale window based on RMM index, we obtained a clear MJO signal in vertical velocity, wind and temperature fields. These three composited fields are found to be coupled together and propagate eastward from the Indian Ocean until they hit the dateline, where abrupt changes occur---the vertical velocity and temperature anomalies decay gradually, while the wind anomalies keep travelling into the Western Hemisphere. An observation is that the span of the wind anomalies extends to the whole globe after crossing the dateline, but before that they are almost confined to the Eastern Hemisphere and Eastern Pacific. We hence divided the whole MJO processes into two distinct state --- phases 2 and 4, according to the reach of its wind anomalies.

To deepen the understanding of the MJO multiscale dynamics, multiscale energy budgets of phases 2 and 4 of the MJO processes have been analyzed within the framework of the multiscale energetics analysis as developed by Liang (2016) in a rigorous sense. For phase 4, there are two KE centers existing at the eastern and western flanks of the convection center over the Eastern Hemisphere. Energy budgets show that pressure gradient work contributes to the KE center at the east of the convection, somewhat reminding us of the Gill model forced by regional convection. However, further analysis shows that this center loses KE to low-frequency window through canonical transfer processes. What’s more, the KE transfer from the low-frequency scale window to the intraseasonal scale window, i.e., the measure of local barotropic instability, is the main KE source for the center at the west of the convection; that is to say, the wind variabilities there is not a simple free Rossby wave as revealed in the Gill model. These findings here provide some evidence for an argument that Gill model cannot explain all the aspects of MJO. KE transports are sinks of the KE at the two centers, while buoyancy conversion contributes KE to them in the lower layer of the centers but consumes

Accepted for publication in *Journal of Climate*. DOI 10.1175/JCLI-D-23-0332.1.

KE in the upper layer. The KE transfer from the high-frequency window to the intraseasonal scale window is almost negative everywhere; that is to say, the energy transfer between the two windows is forward, though insignificant compared to other processes. Distinctly different from phase 4, there are four KE centers covering the whole globe for phase 2. For convenience, they are, by location, referred to as India-Ocean center, Western-Pacific center, Eastern-Pacific center and Atlantic center, respectively. Energy budgets show that pressure gradient work is the main mechanism by which the Western-Pacific center gains KE, while the other three centers mainly gain KE via the canonical KE transfer from the background flow, i.e., through barotropic instability. In detail, barotropic instability processes are much stronger at the two centers over the Western Hemisphere than that at the India-Ocean center. This demonstrates that MJO processes are under stronger modulation by the low-frequency processes over the Western Hemisphere. Our results here show that the radiated energy from the convection center over the Eastern Hemisphere is not the only source of the MJO wind variabilities over the Western Hemisphere; barotropic instability provides a substantial part of energy for their maintenance. A careful analysis of the KE cascade over the Pacific Ocean tells us that the low-frequency variabilities behave like a “bridge” taking the MJO signal across the Pacific. More specifically, MJO stores its energy into the low-frequency window over the western Pacific, and then the low-frequency window releases the part of energy back to the MJO window over the eastern Pacific. Another interesting observation is that there exists evident difference between the KE transport processes of MJO over the Eastern Hemisphere and the Western Hemisphere: the Western-Pacific center and India-Ocean center over the Eastern Hemisphere are sinks of KE, similar to that in phase 4, while shown up at the other two centers over the Western Hemisphere are dipolar patterns, which facilitate the eastward propagation of MJO, and may partly account for the faster propagation over the Western Hemisphere than that over the Eastern Hemisphere.

By analyzing the multiscale APE budget, it is found that the temperature anomalies on intraseasonal scale window could be affected by dynamical processes. Temperature anomalies appear only over the Eastern Hemisphere, whether it be in phase 4 or in phase 2. The two dynamical processes, APE transport and canonical APE transfer from the low-frequency scale window to the intraseasonal scale window, facilitate the formation and maintenance of the temperature anomalies, but buoyancy conversion plays a negative role----it converts APE to KE and thus consumes the temperature anomalies. It should be pointed that our results are consistent with the previous studies, which show that diabatic heating is

Accepted for publication in *Journal of Climate*. DOI 10.1175/JCLI-D-23-0332.1.

important to MJO dynamics (e.g., Hagos et al. 2011). The diabatic heating is included in the residual term here, which also show a significant contribution to the APE sinks/sources of MJO (Figs. 7-8). Numerical biases may also contribute to the residual term here.

All in all, our findings here have provided new evidence supporting the opinion that the evolution of MJO is evidently modulated by multiscale interactions. This is quite different from the assertion (e.g., Zhou et al., 2012) that MJO is actually a linear process and scale-interactions are negligible. We also demonstrate that it is the interaction with low-frequency flow, other than the interaction with higher frequency scales as proposed by Majda et al. (2009, 2011), that plays an important role. In summary, we have found in this paper that multiscale interactions give new insights into the MJO processes from the following four aspects. The most fundamental one is that MJO extracts KE from the low-frequency flow to fuel itself during its lifetime. Secondly, the wind anomalies crossing the dateline into the Western Hemisphere are not radiated free Kelvin waves as proposed in previous works (e.g., Hendon and Salby 1994); they are instead forced ones by the background flow through multiscale interaction. Thirdly, we have found that multiscale interaction can behave as a "bridge" which takes MJO across the Pacific Ocean. Finally, multiscale interaction contributes to the formation and maintenance of the temperature anomalies of MJO.

Acknowledgments.

We are grateful to Dr. Daehyun Kim and an anonymous referee for their help with this manuscript. Particularly, the annonymous referee's advice on the potential role of QBO-MJO interaction is appreciated. This study was partially supported by National Natural Science Foundation of China under Grants 42005052, 41975064, and 42230105, by Southern Marine Science and Engineering Guangdong Laboratory (Zhuhai) through the Startup Foundation (313022003, 313022005), by Fudan University through the Startup Foundation, by Shanghai B & R Joint Laboratory Project (#22230750300), and by Shanghai International Science and Technology Partnership Project (#21230780200).

Data Availability Statement.

The ERA-interim datasets in this study are from https://apps.ecmwf.int/datasets/data/interim-full-daily/levtype=pl/, and the RMM index from http://www.bom.gov.au/climate/mjo/graphics/rmm.74toRealtime.txt. The Outgoing

Accepted for publication in *Journal of Climate*. DOI 10.1175/JCLI-D-23-0332.1.

Longwave Radiation dataset in this study can be downloaded from ftp://ftp.cdc.noaa.gov/Datasets/interp_OLR/olr.day.mean.nc.

APPENDIX

Dynamical symmetry between opposite phases of MJO

MJO is well-known to have two kinds of phases, which is related to enhanced and suppressed convections. This property is illustrated by the opposite behaviors of phases 2 and 6 (as well as phases 4 and 8) in this study. An interesting observation is that the opposite phases are dynamically identical. Figs. A1-A4 are shown here and used to be compared with Figs. 5-8, respectively. It is clearly that the multiscale processes controlling the either the KE and APE of MJO in phases 2 and 6 (as well as phases 4 and 8) are almost the same. In other words, MJO is dynamically symmetric between opposite phases.

Accepted for publication in *Journal of Climate*. DOI 10.1175/JCLI-D-23-0332.1.

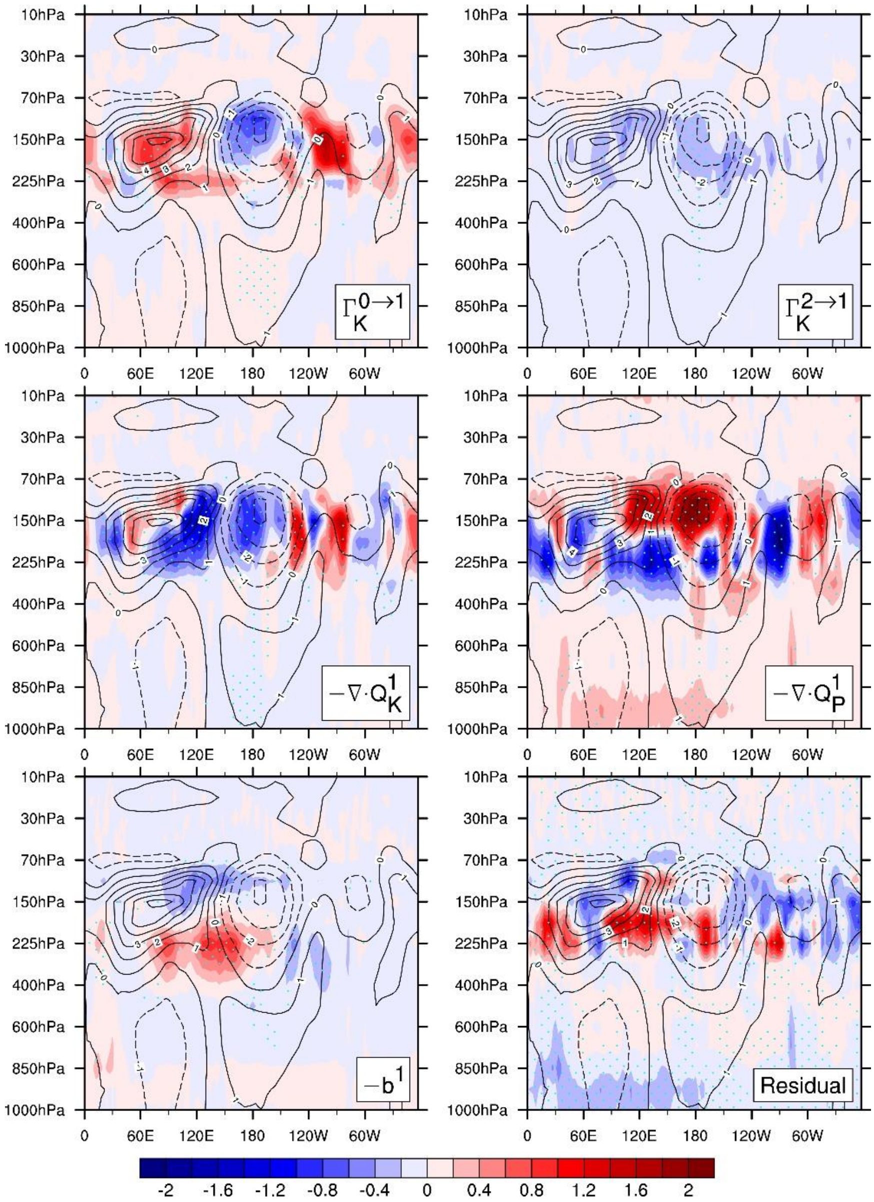

Fig. A1. As in Fig. 5, but for phase 8.

Accepted for publication in *Journal of Climate*. DOI 10.1175/JCLI-D-23-0332.1.

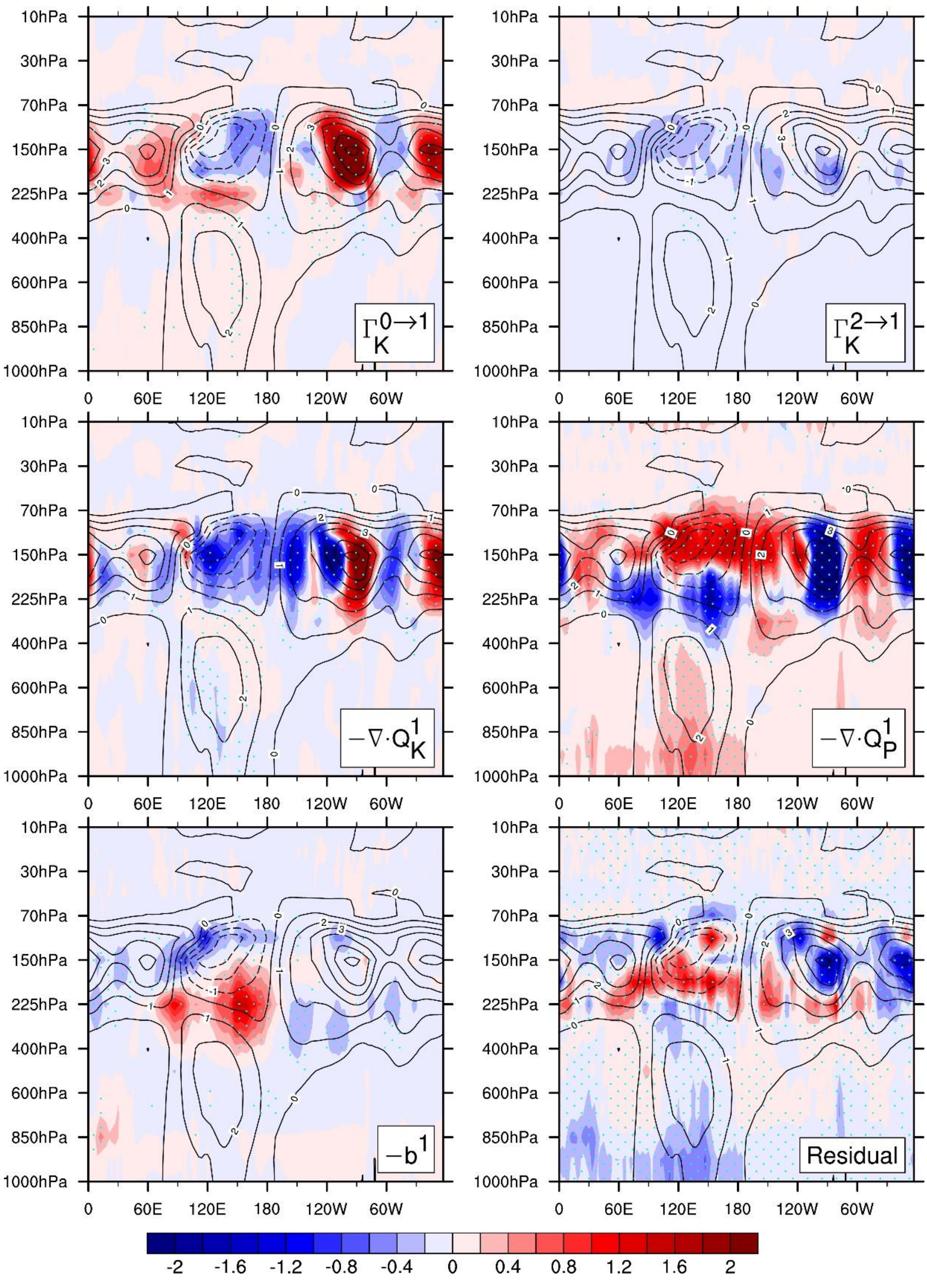

Fig. A2. As in Fig. 6, but for Phase 6

Accepted for publication in *Journal of Climate*. DOI 10.1175/JCLI-D-23-0332.1.

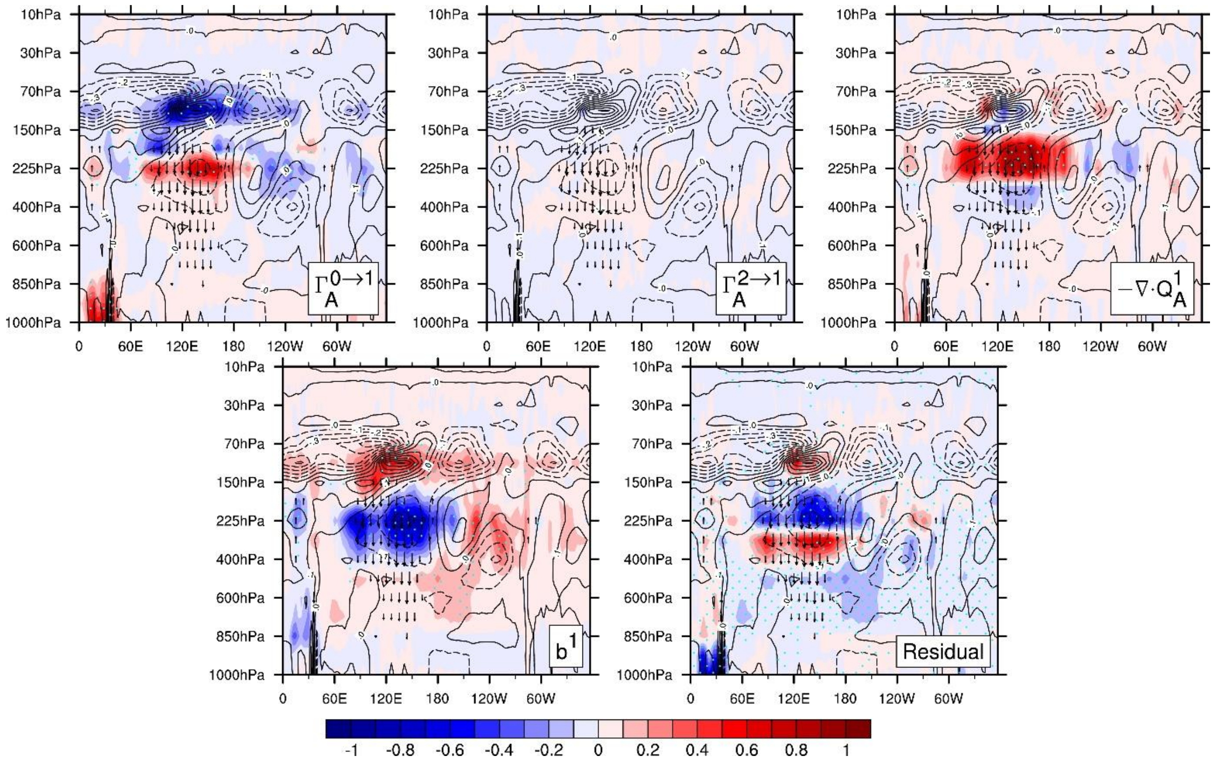

Fig. A3. As in Fig. 7, but for phase 8.

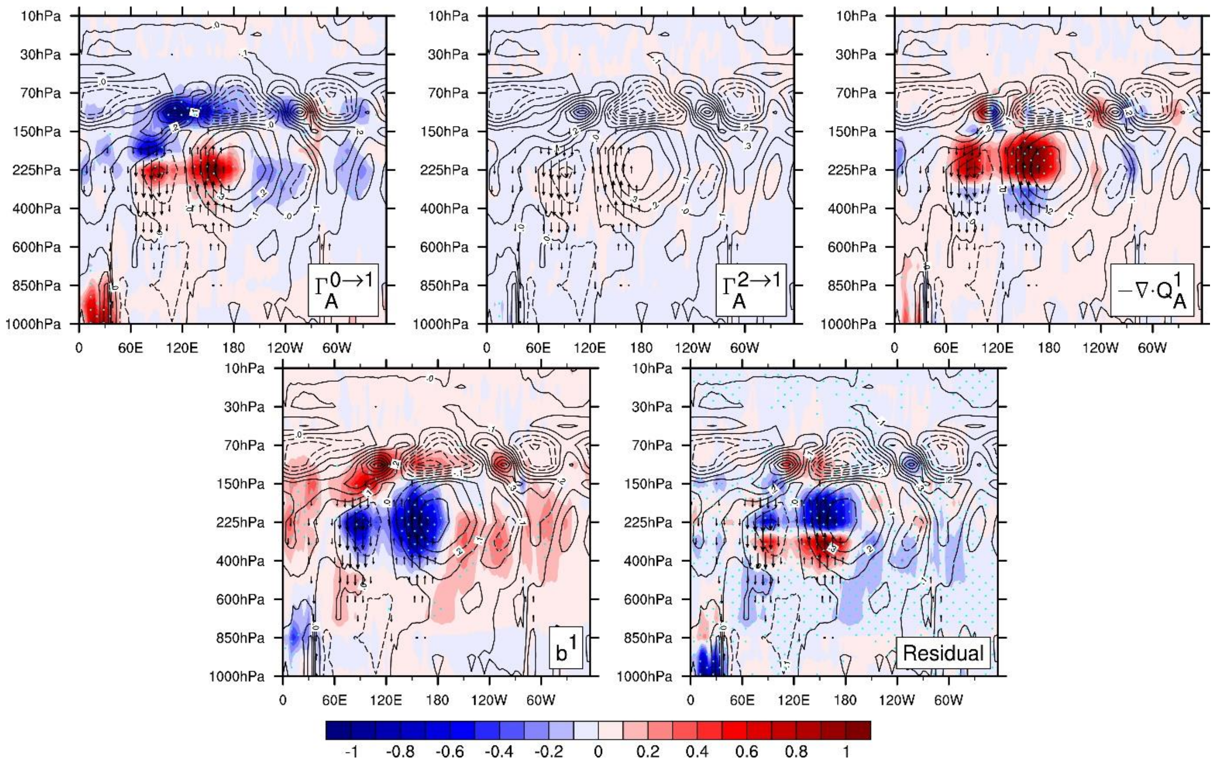

Fig. A4. As in Fig. 8, but for phase 6.

REFERENCES

Accepted for publication in *Journal of Climate*. DOI 10.1175/JCLI-D-23-0332.1.

Adames, Á. F., and J. M. Wallace, 2014a: Three-Dimensional Structure and Evolution of the Vertical Velocity and Divergence Fields in the MJO. *Journal of Atmospheric Sciences*, **71**, 4661–4681, https://doi.org/10.1175/JAS-D-14-0091.1.

——, and ——, 2014b: Three-Dimensional Structure and Evolution of the MJO and Its Relation to the Mean Flow. *Journal of the Atmospheric Sciences*, **71**, 2007–2026, https://doi.org/10.1175/JAS-D-13-0254.1.

——, and ——, 2015: Three-Dimensional Structure and Evolution of the Moisture Field in the MJO. *J. Atmos. Sci.*, **72**, 3733–3754, https://doi.org/10.1175/JAS-D-15-0003.1.

——, and D. Kim, 2016: The MJO as a Dispersive, Convectively Coupled Moisture Wave: Theory and Observations. *J. Atmos. Sci.*, **73**, 913–941, https://doi.org/10.1175/JAS-D-15-0170.1.

Birch, C. E., S. Webster, S. C. Peatman, D. J. Parker, A. J. Matthews, Y. Li, and M. E. E. Hassim, 2016: Scale Interactions between the MJO and the Western Maritime Continent. *Journal of Climate*, **29**, 2471–2492, https://doi.org/10.1175/JCLI-D-15-0557.1.

Cassou, C., 2008: Intraseasonal interaction between the Madden–Julian Oscillation and the North Atlantic Oscillation. *Nature*, **455**, 523–527, https://doi.org/10.1038/nature07286.

Chang, C.-P., and H. Lim, 1988: Kelvin Wave-CISK: A Possible Mechanism for the 30–50 Day Oscillations. *J. Atmos. Sci.*, **45**, 1709–1720, https://doi.org/10.1175/1520-0469(1988)045<1709:KWCAPM>2.0.CO;2.

Chen, T.-C., and J.-M. Chen, 1995: An Observational Study of the South China Sea Monsoon during the 1979 Summer: Onset and Life Cycle. *Mon. Wea. Rev.*, **123**, 2295–2318, https://doi.org/10.1175/1520-0493(1995)123<2295:AOSOTS>2.0.CO;2.

——, S.-Y. Wang, M.-C. Yen, and A. J. Clark, 2009: Impact of the Intraseasonal Variability of the Western North Pacific Large-Scale Circulation on Tropical Cyclone Tracks. *Wea. Forecasting*, **24**, 646–666, https://doi.org/10.1175/2008WAF2222186.1.

Chi, Y., F. Zhang, W. Li, J. He, and Z. Guan, 2015: Correlation between the Onset of the East Asian Subtropical Summer Monsoon and the Eastward Propagation of the Madden–Julian Oscillation. *J. Atmos. Sci.*, **72**, 1200–1214, https://doi.org/10.1175/JAS-D-14-0038.1.

Dee, D. P., and Coauthors, 2011: The ERA-Interim reanalysis: configuration and performance of the data assimilation system. *Quarterly Journal of the Royal Meteorological Society*, **137**, 553–597, https://doi.org/10.1002/qj.828.

Dubey, S., T. N. Krishnamurti, and V. Kumar, 2018: On scale interactions between the MJO and synoptic scale. *Quarterly Journal of the Royal Meteorological Society*, **144**, 2727–2747, https://doi.org/10.1002/qj.3400.

Accepted for publication in *Journal of Climate*. DOI 10.1175/JCLI-D-23-0332.1.

Emanuel, K. A., 1987: An Air-Sea Interaction Model of Intraseasonal Oscillations in the Tropics. *J. Atmos. Sci.*, **44**, 2324–2340, https://doi.org/10.1175/1520-0469(1987)044<2324:AASIMO>2.0.CO;2.

Fuchs, Z., and D. J. Raymond, 2005: Large-Scale Modes in a Rotating Atmosphere with Radiative–Convective Instability and WISHE. *J. Atmos. Sci.*, **62**, 4084–4094, https://doi.org/10.1175/JAS3582.1.

Hagos, S., L. R. Leung, and J. Dudhia, 2011: Thermodynamics of the Madden–Julian Oscillation in a Regional Model with Constrained Moisture. *J. Atmos. Sci.*, **68**, 1974–1989, https://doi.org/10.1175/2011JAS3592.1.

Hagos, S. M., C. Zhang, Z. Feng, C. D. Burleyson, C. D. Mott, B. Kerns, J. J. Benedict, and M. N. Martini, 2016: The impact of the diurnal cycle on the propagation of Madden-Julian Oscillation convection across the Maritime Continent. *Journal of Advances in Modeling Earth Systems*, **8**, 1552–1564, https://doi.org/10.1002/2016MS000725.

Hamill, T. M., and G. N. Kiladis, 2014: Skill of the MJO and Northern Hemisphere Blocking in GEFS Medium-Range Reforecasts. *Mon. Wea. Rev.*, **142**, 868–885, https://doi.org/10.1175/MWR-D-13-00199.1.

Hayashi, M., and H. Itoh, 2017: A New Mechanism of the Slow Eastward Propagation of Unstable Disturbances with Convection in the Tropics: Implications for the MJO. *Journal of the Atmospheric Sciences*, **74**, 3749–3769, https://doi.org/10.1175/JAS-D-16-0300.1.

Henderson, S. A., E. D. Maloney, and E. A. Barnes, 2016: The Influence of the Madden–Julian Oscillation on Northern Hemisphere Winter Blocking. *J. Climate*, **29**, 4597–4616, https://doi.org/10.1175/JCLI-D-15-0502.1.

Hendon, H. H., and B. Liebmann, 1990: The Intraseasonal (30–50 day) Oscillation of the Australian Summer Monsoon. *J. Atmos. Sci.*, **47**, 2909–2924, https://doi.org/10.1175/1520-0469(1990)047<2909:TIDOOT>2.0.CO;2.

——, and M. L. Salby, 1994: The Life Cycle of the Madden–Julian Oscillation. *J. Atmos. Sci.*, **51**, 2225–2237, https://doi.org/10.1175/1520-0469(1994)051<2225:TLCOTM>2.0.CO;2.

——, and ——, 1996: Planetary-Scale Circulations Forced by Intraseasonal Variations of Observed Convection. *J. Atmos. Sci.*, **53**, 1751–1758, https://doi.org/10.1175/1520-0469(1996)053<1751:PSCFBI>2.0.CO;2.

Hsieh Y.-P., Chen S.-J., Chang I.-L., and Huang Y.-L., 1963: A preliminarily statistic and synoptic study about the basic currents over southeastern Asia and the initiation of typhoon (in Chinese). *Acta Meteor. Sin.*, **33**, 206–217, https://doi.org/10.11676/qxxb1963.020.

Hsu, P., T. Li, and C.-H. Tsou, 2010: Interactions between Boreal Summer Intraseasonal Oscillations and Synoptic-Scale Disturbances over the Western North Pacific. Part I: Energetics Diagnosis. *J. Climate*, **24**, 927–941, https://doi.org/10.1175/2010JCLI3833.1.

File generated with AMS Word template 2.0

Accepted for publication in *Journal of Climate*. DOI 10.1175/JCLI-D-23-0332.1.

Jiang, X., and Coauthors, 2015: Vertical structure and physical processes of the Madden-Julian oscillation: Exploring key model physics in climate simulations. *Journal of Geophysical Research: Atmospheres*, **120**, 4718–4748, https://doi.org/10.1002/2014JD022375.

Kessler, W. S., and R. Kleeman, 2000: Rectification of the Madden–Julian Oscillation into the ENSO Cycle. *J. Climate*, **13**, 3560–3575, https://doi.org/10.1175/1520-0442(2000)013<3560:ROTMJO>2.0.CO;2.

——, M. J. McPhaden, and K. M. Weickmann, 1995: Forcing of intraseasonal Kelvin waves in the equatorial Pacific. *Journal of Geophysical Research: Oceans*, **100**, 10613–10631, https://doi.org/10.1029/95JC00382.

Kiladis, G. N., K. H. Straub, and P. T. Haertel, 2005: Zonal and Vertical Structure of the Madden–Julian Oscillation. *J. Atmos. Sci.*, **62**, 2790–2809, https://doi.org/10.1175/JAS3520.1.

——, J. Dias, K. H. Straub, M. C. Wheeler, S. N. Tulich, K. Kikuchi, K. M. Weickmann, and M. J. Ventrice, 2014: A Comparison of OLR and Circulation-Based Indices for Tracking the MJO. *Monthly Weather Review*, **142**, 1697–1715, https://doi.org/10.1175/MWR-D-13-00301.1.

Kim, J.-H., C.-H. Ho, H.-S. Kim, C.-H. Sui, and S. K. Park, 2008: Systematic Variation of Summertime Tropical Cyclone Activity in the Western North Pacific in Relation to the Madden–Julian Oscillation. *J. Climate*, **21**, 1171–1191, https://doi.org/10.1175/2007JCLI1493.1.

Knutson, T. R., and K. M. Weickmann, 1987: 30–60 Day Atmospheric Oscillations: Composite Life Cycles of Convection and Circulation Anomalies. *Mon. Wea. Rev.*, **115**, 1407–1436, https://doi.org/10.1175/1520-0493(1987)115<1407:DAOCLC>2.0.CO;2.

——, ——, and J. E. Kutzbach, 1986: Global-Scale Intraseasonal Oscillations of Outgoing Longwave Radiation and 250 mb Zonal Wind during Northern Hemisphere Summer. *Monthly Weather Review*, **114**, 605–623, https://doi.org/10.1175/1520-0493(1986)114<0605:GSIOOO>2.0.CO;2.

Krishnamurti, T. N., and D. Subrahmanyam, 1982: The 30–50 Day Mode at 850 mb During MONEX. *J. Atmos. Sci.*, **39**, 2088–2095, https://doi.org/10.1175/1520-0469(1982)039<2088:TDMAMD>2.0.CO;2.

——, D. R. Chakraborty, N. Cubukcu, L. Stefanova, and T. S. V. Vijaya Kumar, 2003: A mechanism of the Madden–Julian Oscillation based on interactions in the frequency domain. *Quarterly Journal of the Royal Meteorological Society*, **129**, 2559–2590, https://doi.org/10.1256/qj.02.151.

Lau, K.-M., and P. H. Chan, 1986: Aspects of the 40–50 Day Oscillation during the Northern Summer as Inferred from Outgoing Longwave Radiation. *Mon. Wea. Rev.*, **114**, 1354–1367, https://doi.org/10.1175/1520-0493(1986)114<1354:AOTDOD>2.0.CO;2.

Accepted for publication in *Journal of Climate*. DOI 10.1175/JCLI-D-23-0332.1.

Lau, K.-M., and L. Peng, 1987: Origin of Low-Frequency (Intraseasonal) Oscillations in the Tropical Atmosphere. Part I: Basic Theory. *J. Atmos. Sci.*, **44**, 950–972, https://doi.org/10.1175/1520-0469(1987)044<0950:OOLFOI>2.0.CO;2.

Li, T., L. Wang, M. Peng, B. Wang, C. Zhang, W. Lau, and H.-C. Kuo, 2018: A Paper on the Tropical Intraseasonal Oscillation Published in 1963 in a Chinese Journal. *Bulletin of the American Meteorological Society*, **99**, 1765–1779, https://doi.org/10.1175/BAMS-D-17-0216.1.

Liang, X. S., 2016: Canonical Transfer and Multiscale Energetics for Primitive and Quasigeostrophic Atmospheres. *J. Atmos. Sci.*, **73**, 4439–4468, https://doi.org/10.1175/JAS-D-16-0131.1.

——, and A. R. Robinson, 2005: Localized multiscale energy and vorticity analysis: I. Fundamentals. *Dynamics of Atmospheres and Oceans*, **38**, 195–230, https://doi.org/10.1016/j.dynatmoce.2004.12.004.

——, and D. Anderson, 2007: Multiscale Window Transform. *Multiscale Model. Simul.*, **6**, 437–467, https://doi.org/10.1137/06066895X.

Liebmann, B., and C. A. Smith, 1996: Description of a Complete (Interpolated) Outgoing Longwave Radiation Dataset. *Bulletin of the American Meteorological Society*, **77**, 1275–1277.

——, H. H. Hendon, and J. D. Glick, 1994: The Relationship Between Tropical Cyclones of the Western Pacific and Indian Oceans and the Madden-Julian Oscillation. *Journal of the Meteorological Society of Japan. Ser. II*, **72**, 401–412, https://doi.org/10.2151/jmsj1965.72.3_401.

Lindzen, R. S., 1974: Wave-CISK in the Tropics. *J. Atmos. Sci.*, **31**, 156–179, https://doi.org/10.1175/1520-0469(1974)031<0156:WCITT>2.0.CO;2.

Lorenz, E. N., 1955: Available Potential Energy and the Maintenance of the General Circulation. *Tellus*, **7**, 157–167, https://doi.org/10.1111/j.2153-3490.1955.tb01148.x.

Ma, J., and X. S. Liang, 2017: Multiscale Dynamical Processes Underlying the Wintertime Atlantic Blockings. *J. Atmos. Sci.*, **74**, 3815–3831, https://doi.org/10.1175/JAS-D-16-0295.1.

——, and ——, 2023a: Upstream-downstream asymmetry in multiscale interaction underlying the Northern Hemisphere atmospheric blockings. *Journal of the Atmospheric Sciences*, **1**, https://doi.org/10.1175/JAS-D-22-0220.1.

——, and ——, 2023b: Distinctly Different Dynamical Processes in Maintaining the Intraseasonal NAO+ and NAO−. *Geophysical Research Letters*, **50**, e2023GL103351, https://doi.org/10.1029/2023GL103351.

Madden, R. A., and P. R. Julian, 1971: Detection of a 40–50 Day Oscillation in the Zonal Wind in the Tropical Pacific. *Journal of the Atmospheric Sciences*, **28**, 702–708, https://doi.org/10.1175/1520-0469(1971)028<0702:DOADOI>2.0.CO;2.

Accepted for publication in *Journal of Climate*. DOI 10.1175/JCLI-D-23-0332.1.

——, and ——, 1972: Description of Global-Scale Circulation Cells in the Tropics with a 40–50 Day Period. *J. Atmos. Sci.*, **29**, 1109–1123, https://doi.org/10.1175/1520-0469(1972)029<1109:DOGSCC>2.0.CO;2.

Majda, A. J., and J. A. Biello, 2003: The Nonlinear Interaction of Barotropic and Equatorial Baroclinic Rossby Waves. *J. Atmos. Sci.*, **60**, 1809–1821, https://doi.org/10.1175/1520-0469(2003)060<1809:TNIOBA>2.0.CO;2.

Majda, A. J., and S. N. Stechmann, 2009: The skeleton of tropical intraseasonal oscillations. *Proceedings of the National Academy of Sciences*, **106**, 8417–8422, https://doi.org/10.1073/pnas.0903367106.

Majda, A. J., and S. N. Stechmann, 2011: Nonlinear Dynamics and Regional Variations in the MJO Skeleton. *J. Atmos. Sci.*, **68**, 3053–3071, https://doi.org/10.1175/JAS-D-11-053.1.

Maloney, E. D., and D. L. Hartmann, 1998: Frictional Moisture Convergence in a Composite Life Cycle of the Madden–Julian Oscillation. *Journal of Climate*, **11**, 2387–2403, https://doi.org/10.1175/1520-0442(1998)011<2387:FMCIAC>2.0.CO;2.

——, and ——, 2000: Modulation of Eastern North Pacific Hurricanes by the Madden–Julian Oscillation. *J. Climate*, **13**, 1451–1460, https://doi.org/10.1175/1520-0442(2000)013<1451:MOENPH>2.0.CO;2.

——, and ——, 2001: The Madden–Julian Oscillation, Barotropic Dynamics, and North Pacific Tropical Cyclone Formation. Part I: Observations. *Journal of the Atmospheric Sciences*, **58**, 2545–2558, https://doi.org/10.1175/1520-0469(2001)058<2545:TMJOBD>2.0.CO;2.

Matthews, A. J., 2000: Propagation mechanisms for the Madden-Julian Oscillation. *Quarterly Journal of the Royal Meteorological Society*, **126**, 2637–2651, https://doi.org/10.1002/qj.49712656902.

——, 2004: Intraseasonal Variability over Tropical Africa during Northern Summer. *J. Climate*, **17**, 2427–2440, https://doi.org/10.1175/1520-0442(2004)017<2427:IVOTAD>2.0.CO;2.

Mo, K. C., and R. W. Higgins, 1998: Tropical Convection and Precipitation Regimes in the Western United States. *J. Climate*, **11**, 2404–2423, https://doi.org/10.1175/1520-0442(1998)011<2404:TCAPRI>2.0.CO;2.

Moore, A. M., and R. Kleeman, 1999: Stochastic Forcing of ENSO by the Intraseasonal Oscillation. *J. Climate*, **12**, 1199–1220, https://doi.org/10.1175/1520-0442(1999)012<1199:SFOEBT>2.0.CO;2.

Moore, R. W., O. Martius, and T. Spengler, 2010: The Modulation of the Subtropical and Extratropical Atmosphere in the Pacific Basin in Response to the Madden–Julian Oscillation. *Mon. Wea. Rev.*, **138**, 2761–2779, https://doi.org/10.1175/2010MWR3194.1.

Accepted for publication in *Journal of Climate*. DOI 10.1175/JCLI-D-23-0332.1.

Neelin, J. D., I. M. Held, and K. H. Cook, 1987: Evaporation-Wind Feedback and Low-Frequency Variability in the Tropical Atmosphere. *J. Atmos. Sci.*, **44**, 2341–2348, https://doi.org/10.1175/1520-0469(1987)044<2341:EWFALF>2.0.CO;2.

Paegle, J. N., L. A. Byerle, and K. C. Mo, 2000: Intraseasonal Modulation of South American Summer Precipitation. *Mon. Wea. Rev.*, **128**, 837–850, https://doi.org/10.1175/1520-0493(2000)128<0837:IMOSAS>2.0.CO;2.

Plumb, R. A., 1983: A New Look at the Energy Cycle. *J. Atmos. Sci.*, **40**, 1669–1688, https://doi.org/10.1175/1520-0469(1983)040<1669:ANLATE>2.0.CO;2.

Ray, P., and T. Li, 2013: Relative Roles of Circumnavigating Waves and Extratropics on the MJO and Its Relationship with the Mean State. *Journal of the Atmospheric Sciences*, **70**, 876–893, https://doi.org/10.1175/JAS-D-12-0153.1.

——, C. Zhang, M. W. Moncrieff, J. Dudhia, J. M. Caron, L. Ruby Leung, and C. Bruyere, 2011: Role of the atmospheric mean state on the initiation of the Madden-Julian oscillation in a tropical channel model. *Clim Dyn*, **36**, 161–184, https://doi.org/10.1007/s00382-010-0859-2.

Raymond, D. J., and Ž. Fuchs, 2009: Moisture Modes and the Madden–Julian Oscillation. *J. Climate*, **22**, 3031–3046, https://doi.org/10.1175/2008JCLI2739.1.

Roundy, P. E., 2012: Observed Structure of Convectively Coupled Waves as a Function of Equivalent Depth: Kelvin Waves and the Madden–Julian Oscillation. *Journal of the Atmospheric Sciences*, **69**, 2097–2106, https://doi.org/10.1175/JAS-D-12-03.1.

——, 2014: Some Aspects of Western Hemisphere Circulation and the Madden–Julian Oscillation. *J. Atmos. Sci.*, **71**, 2027–2039, https://doi.org/10.1175/JAS-D-13-0210.1.

Sakaeda, N., and P. E. Roundy, 2015: The Development of Upper-Tropospheric Wind over the Western Hemisphere in Association with MJO Convective Initiation. *J. Atmos. Sci.*, **72**, 3138–3160, https://doi.org/10.1175/JAS-D-14-0293.1.

Salby, M. L., R. R. Garcia, and H. H. Hendon, 1994: Planetary-Scale Circulations in the Presence of Climatological and Wave-Induced Heating. *Journal of the Atmospheric Sciences*, **51**, 2344–2367, https://doi.org/10.1175/1520-0469(1994)051<2344:PSCITP>2.0.CO;2.

Sherwood, S. C., T. Horinouchi, and H. A. Zeleznik, 2003: Convective Impact on Temperatures Observed near the Tropical Tropopause. *Journal of the Atmospheric Sciences*, **60**, 1847–1856, https://doi.org/10.1175/1520-0469(2003)060<1847:CIOTON>2.0.CO;2.

Sobel, A., and E. Maloney, 2012: An Idealized Semi-Empirical Framework for Modeling the Madden–Julian Oscillation. *J. Atmos. Sci.*, **69**, 1691–1705, https://doi.org/10.1175/JAS-D-11-0118.1.

Sobel, A. H., and D. Kim, 2012: The MJO-Kelvin wave transition. *Geophysical Research Letters*, **39**, https://doi.org/10.1029/2012GL053380.

Accepted for publication in *Journal of Climate*. DOI 10.1175/JCLI-D-23-0332.1.

Straub, K. H., G. N. Kiladis, and P. E. Ciesielski, 2006: The role of equatorial waves in the onset of the South China Sea summer monsoon and the demise of El Niño during 1998. *Dynamics of Atmospheres and Oceans*, **42**, 216–238, https://doi.org/10.1016/j.dynatmoce.2006.02.005.

Tang, Y., and B. Yu, 2008: MJO and its relationship to ENSO. *Journal of Geophysical Research: Atmospheres*, **113**, https://doi.org/10.1029/2007JD009230.

Tian, B., D. E. Waliser, and E. J. Fetzer, 2006: Modulation of the diurnal cycle of tropical deep convective clouds by the MJO. *Geophysical Research Letters*, **33**, https://doi.org/10.1029/2006GL027752.

Tong, H. W., J. C. L. Chan, and W. Zhou, 2009: The role of MJO and mid-latitude fronts in the South China Sea summer monsoon onset. *Clim Dyn*, **33**, 827–841, https://doi.org/10.1007/s00382-008-0490-7.

Wang, B., 1988: Dynamics of Tropical Low-Frequency Waves: An Analysis of the Moist Kelvin Wave. *J. Atmos. Sci.*, **45**, 2051–2065, https://doi.org/10.1175/1520-0469(1988)045<2051:DOTLFW>2.0.CO;2.

Wang, B., and H. Rui, 1990: Synoptic climatology of transient tropical intraseasonal convection anomalies: 1975–1985. *Meteorl. Atmos. Phys.*, **44**, 43–61, https://doi.org/10.1007/BF01026810.

Wang, B., and F. Liu, 2011: A Model for Scale Interaction in the Madden–Julian Oscillation. *Journal of the Atmospheric Sciences*, **68**, 2524–2536, https://doi.org/10.1175/2011JAS3660.1.

——, ——, and G. Chen, 2016: A trio-interaction theory for Madden–Julian oscillation. *Geosci. Lett.*, **3**, 1–16, https://doi.org/10.1186/s40562-016-0066-z.

Wang, L., T. Li, and L. Chen, 2019: Modulation of the Madden–Julian oscillation on the energetics of wintertime synoptic-scale disturbances. *Clim Dyn*, **52**, 4861–4871, https://doi.org/10.1007/s00382-018-4447-1.

Wang, S., and A. H. Sobel, 2022: A Unified Moisture Mode Theory for the Madden–Julian Oscillation and the Boreal Summer Intraseasonal Oscillation. *Journal of Climate*, **35**, 1267–1291, https://doi.org/10.1175/JCLI-D-21-0361.1.

——, D. Ma, A. H. Sobel, and M. K. Tippett, 2018: Propagation Characteristics of BSISO Indices. *Geophysical Research Letters*, **45**, 9934–9943, https://doi.org/10.1029/2018GL078321.

Weickmann, K. M., 1991: El Niño/Southern Oscillation and Madden-Julian (30–60 day) oscillations during 1981–1982. *Journal of Geophysical Research: Oceans*, **96**, 3187–3195, https://doi.org/10.1029/90JD01832.

Wheeler, M. C., and H. H. Hendon, 2004: An All-Season Real-Time Multivariate MJO Index: Development of an Index for Monitoring and Prediction. *Mon. Wea. Rev.*, **132**, 1917–1932, https://doi.org/10.1175/1520-0493(2004)132<1917:AARMMI>2.0.CO;2.

Accepted for publication in *Journal of Climate*. DOI 10.1175/JCLI-D-23-0332.1.

Xu, F., and X. S. Liang, 2020: The Synchronization between the Zonal Jet Stream and Temperature Anomalies Leads to an Extremely Freezing North America in January 2019. *Geophysical Research Letters*, **47**, e2020GL089689, https://doi.org/10.1029/2020GL089689.

Yang, D., and A. P. Ingersoll, 2013: Triggered Convection, Gravity Waves, and the MJO: A Shallow-Water Model. *Journal of the Atmospheric Sciences*, **70**, 2476–2486, https://doi.org/10.1175/JAS-D-12-0255.1.

Yang, Y., R. H. Weisberg, Y. Liu, and X. San Liang, 2020: Instabilities and Multiscale Interactions Underlying the Loop Current Eddy Shedding in the Gulf of Mexico. *J. Phys. Oceanogr.*, **50**, 1289–1317, https://doi.org/10.1175/JPO-D-19-0202.1.

Yano, J.-I., and K. Emanuel, 1991: An Improved Model of the Equatorial Troposphere and Its Coupling with the Stratosphere. *J. Atmos. Sci.*, **48**, 377–389, https://doi.org/10.1175/1520-0469(1991)048<0377:AIMOTE>2.0.CO;2.

——, and J. J. Tribbia, 2017: Tropical Atmospheric Madden–Julian Oscillation: A Strongly Nonlinear Free Solitary Rossby Wave? *Journal of the Atmospheric Sciences*, **74**, 3473–3489, https://doi.org/10.1175/JAS-D-16-0319.1.

Zhang, C., and M. Dong, 2004: Seasonality in the Madden–Julian Oscillation. *Journal of Climate*, **17**, 3169–3180, https://doi.org/10.1175/1520-0442(2004)017<3169:SITMO>2.0.CO;2.

Zhao, Y.-B., X. S. Liang, Z. Guan, and K. I. Hodges, 2019: The asymmetric eddy–background flow interaction in the North Pacific storm track. *Quarterly Journal of the Royal Meteorological Society*, **145**, 575–596, https://doi.org/10.1002/qj.3453.

Zhou, L., A. H. Sobel, and R. Murtugudde, 2012: Kinetic Energy Budget for the Madden–Julian Oscillation in a Multiscale Framework. *J. Climate*, **25**, 5386–5403, https://doi.org/10.1175/JCLI-D-11-00339.1.

Zhou, W., and J. C. L. Chan, 2005: Intraseasonal oscillations and the South China Sea summer monsoon onset. *International Journal of Climatology*, **25**, 1585–1609, https://doi.org/10.1002/joc.1209.

Zhu, Y., T. Li, M. Zhao, and T. Nasuno, 2019: Interaction between the MJO and High-Frequency Waves over the Maritime Continent in Boreal Winter. *Journal of Climate*, **32**, 3819–3835, https://doi.org/10.1175/JCLI-D-18-0511.1.

Accepted for publication in *Journal of Climate*. DOI 10.1175/JCLI-D-23-0332.1.